Published in : Angewandte Chemie (2018), vol. 57, n°11, pp. 2934–2937
DOI: 10.1002/anie.201712347
Status : Postprint (Author's version)

ORGANOMETALLIC-MEDIATED RADICAL POLYMERIZATION OF VINYLIDENE FLUORIDE

Sanjib Banerjee, Vincent Ladmiral, Antoine Debuigne, Christophe Detrembleur, Rinaldo Poli,* and Bruno Améduri*

Dr. S Banerjee, Dr. V. Ladmiral, Dr. B. Améduri, Ingénierie et Architectures Macromoléculaires, Institut Charles Gerhardt, UMR 5253 CNRS, UM, ENSCM, Place Eugène Bataillon, 34095 Montpellier Cedex 5, France

Dr. A. Debuigne, Dr. C. Detrembleur, Center for Education and Research on Macromolecules (CERM), CESAM Research Unit, University of Liege, Department of Chemistry, Sart-Tilman B6a, 4000 Liege, Belgium

Prof. R. Poli, CNRS, LCC (Laboratoire de Chimie de Coordination) and Université de Toulouse, UPS, INPT, 205 route de Narbonne, BP 44099, 31077 Toulouse Cedex 4, France and Institut Universitaire de France, 1, rue Descartes, 75231, Paris Cedex 05, France

Dr. S. Banerjee, Department of Chemistry, Indian Institute of Technology Bhilai, Raipur 492015, Chhattisgarh, India

Keywords:

Block copolymers, Cobalt, One pot synthesis, Organometallic-mediated radical polymerization, Vinylidene fluoride

Abstract

An unprecedented level of control for the radical polymerization of vinylidene fluoride (VDF), yielding well-defined PVDF (at least up to 14500 $gmol^{-1}$) with low dispersity (≤1.32), was achieved using organometallic-mediated radical polymerization (OMRP) with an organocobalt compound as initiator. The high chain-end fidelity was demonstrated by the synthesis of PVDF- and PVAc-containing di-and triblock copolymers. DFT calculations rationalize the efficient reactivation of both head and tail chain end dormant species.

Published in : Angewandte Chemie (2018), vol. 57, n°11, pp. 2934–2937
DOI: 10.1002/anie.201712347
Status : Postprint (Author's version)

Poly(vinylidene fluoride), PVDF, is the second largest commercially available fluoropolymer after polytetrafluoroethylene (PTFE). It exhibits remarkable properties, such as hydrophobic and oleophobic properties, chemical resistance to acids and solvents, low dielectric constants and excellent weathering.[1] Hence, it finds uses in many high-tech applications in aerospace and aeronautical engineering, coatings,[1d] piezo/ferroelectric devices,[2] backsheets for photovoltaic devices and functional membranes for water treatment.[3] VDF has a reactivity close to those of TFE[1b] and chlorotrifuoroethylene,[4] but it is not explosive and much less toxic.[1c]

Reversible deactivation radical polymerization (RDRP) of VDF has only been achieved using two techniques: 1) iodine transfer polymerization (ITP),[1c,5] and 2) reversible addition fragmentation chain transfer (RAFT) polymerization.[6,7] Both techniques require the use of a radical initiator and a suitable chain transfer agent (CTA), which ensures the reversible degenerative transfer (DT) at the heart of ITP and RAFT. Both were shown to produce relatively well-defined diblock[1c,5b,c, 6c,7] and triblock[1c,5b,c] copolymers. However, the chain defects resulting from head-to-head (HH, -CH_2CF_2-CF_2CH_2-) monomer additions impose limits on the molar masses (M_n) and dispersities ($Đ$) attainable with these techniques, as demonstrated in both ITP[5c] and RAFT[6b] polymerization. Upon transfer to the CTA, the HH additions generate less-reactive species that lead to a slowdown of the degenerative chain transfer, a broadening of the molar mass distribution and a degradation of the control.[6b,c,8] Ideally, a RDRP technique should reactivate both PVDF chain ends at the same rate. Asandei et al.[9] were able to reactivate the -CF_2CH_2-I terminated PVDF chains and to synthesize block copolymers using $Mn_2(CO)_{10}$ and a photoirradiation process in ITP. However, further reactivation to access block copolymer structures was only possible using conventional radical polymerization. Liepins et al.[10] reported the synthesis of PVDF with a low content of HH chain defects using a modified Ziegler–Natta catalyst, while Chung's group[11] used a trialkylborane/oxygen mixture as the initiating system resulting in significant chain defects. However, the controlled nature of these polymerizations was not addressed. In terms of the coordination-insertion strategy for fluorinated alkenes, Jordan et al.[12] described the copolymerization of vinyl fluoride and ethylene using (phosphine-arenesulfonate)Pd(Me)(py) and phosphine bis(arenesulfonate)PdMe(py) catalysts, while Rieger and co-workers reported the copolymerization of 3,3,3-trifluoropropene with ethylene using (phosphinesulfonate)Pd(Me)(DMSO) as catalyst.[13] However, these catalysts did not provide a very good control. To our knowledge, there is no report on the VDF homopolymerization or VDF-olefin copolymerization using this strategy.

Among other RDRP techniques, organometallic-mediated radical polymerization (OMRP), in which a transitionmetal complex reversibly traps the propagating polymer radicals,[14] has been successfully employed for the radical (co)polymerization of less-reactive monomers, including vinyl acetate (VAc)[14a–c] and VAc-ethylene, with $Co^{II}(acac)_2$ (acac=acetylacetonate) as controlling agent.[15] However, this technique has never been used to homopolymerize fluorinated alkenes. We report herein the first example of OMRP of a fluorinated gaseous monomer (VDF) under mild experimental conditions, leading to unprecedented control over the homopolymerization of this monomer (**Scheme 1**). Furthermore, macromolecular engineering was achieved using the in situ generated PVDF-$Co(acac)_2$ macroinitiator to prepare well-defined PVAc- and PVDF-containing diblock- and triblock copolymers (**Scheme S1** in the **Supporting Information**).

Published in : Angewandte Chemie (2018), vol. 57, n°11, pp. 2934–2937
DOI: 10.1002/anie.201712347
Status : Postprint (Author's version)

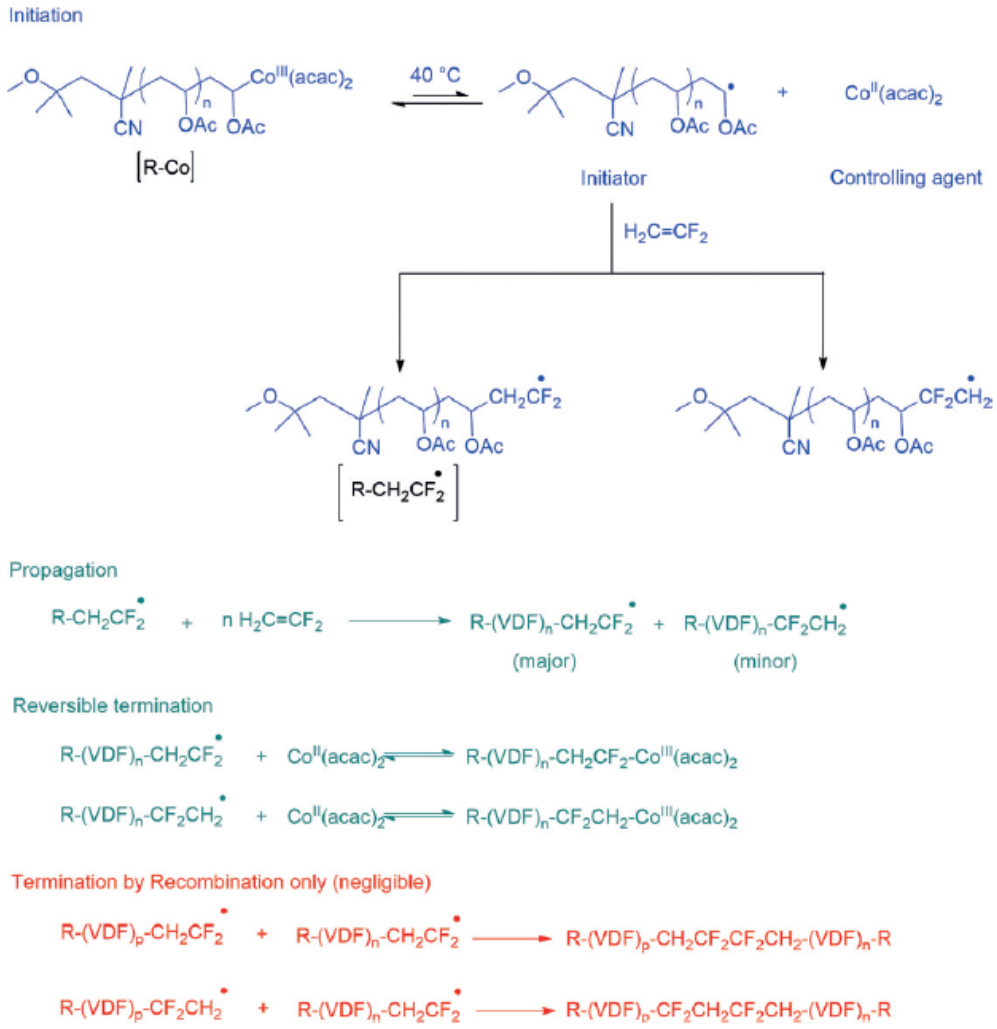

Scheme 1. Mechanism of OMRP of vinylidene fluoride (VDF).

VDF homopolymerizations were carried out in dimethyl carbonate (DMC, a solvent with a low aptitude to transfer H atoms to PVDF radicals and which swells PVDF[1c]) in a Hastelloy (HC 276) autoclave at 408C using the organocobalt initiator, $[R_0(VAc)_{\approx 4}Co^{III}(acac)_2$ as initiator (R_0 =primary radical generated V-70)][16], abbreviated as R-Co^{III}, at three $[VDF]_0/[R\text{-}Co^{III}]_0$ initial molar ratios (100, 200, and 300). Notably, no polymerization was observed when V-70/ $Co^{II}(acac)_2$ was used at 40°C or even at 50°C. This shows that azo initiators are not able to initiate the polymerization of VDF[1c] and justifies the choice of R-Co as the initiating species. The selected temperature was the mildest one allowing to attain a reasonable control. These polymerizations produced PVDFs with higher targeted molar masses (M_n= 5900 to 14 500 $gmol^{-1}$) and lower dispersity values ($Đ \leq 1.32$; P1-P3, **Table S1** and **Figure S1**), lower than those achieved by ITP or RAFT measured under the same conditions.

^{1}H, ^{19}F, and ^{13}C NMR spectroscopy enabled the structural analysis of the synthesized PVDFs, including the chain ends (see details in **Supporting Information**). The recovered polymers, isolated after quenching with TEMPO (see **Supporting Information**, **Figures S2**–**S4**, **P2**, **Table S1**), showed the expected features (normal head-to-tail and reversed head-to-head and tail-to-tail monomer additions) radically polymerized VDF, the -CF_2H and -CH_3 end-groups originating from transfer reactions, the

Published in : Angewandte Chemie (2018), vol. 57, n°11, pp. 2934–2937
DOI: 10.1002/anie.201712347
Status : Postprint (Author's version)

characteristic signals of the oligo(VAc) group from the R-Co initiator (^{1}H NMR, **Figure S2**), and the TEMPO chain end (^{19}F NMR, **Figure 2B** and **Figure S3**). Notably only the R_0-(VAc)$_{\approx 4}$-CH_2CF_2- and not the R_0-(VAc)$_{\approx 4}$-CF_2CH_2- α-chain end could be identified, whereas both -CF_2CH_2-CH_2CF_2-TEMPO and -CH_2CF_2-CH_2CF_2-TEMPO ω-chain ends were visible at -66.5 and -61.5 ppm, respectively. The Supporting Information offers a more detailed discussion of these assignments.

A polymerization kinetic study was carried out through a series of single point experiments (ranging from 0.5 to 24 h, entries 1–7 in **Table S2**) with TEMPO quenching to eliminate the cobalt complex from the polymer chain-end.[17] The VDF conversion was determined gravimetrically, while the M_n and $Đ$ values were assessed by SEC calibrated with poly(methyl methacrylate) standards (**Table S2**). The slope of the "linear" first order kinetic plot (ln([M]$_0$/[M]) vs. time) (**Figure S5**B) yields an apparent propagation rate constant {$k_{p(app)}$)} of 9.6X10^{-6} $^{s-1}$. The "point by point" kinetic study with seven independent runs demonstrates the reproducibility of the system. The SEC traces (**Figure S6**) remained relatively narrow and monomodal throughout the polymerization. The M_n versus conversion plot (**Figure 1**) exhibits a monotonous linear increase, maintaining low $Đ$ values (1.14–1.29), consistent with the features of RDRP.[5c]

The evolutions of the -CF_2CH_2-TEMPO and -CH_2CF_2-TEMPO end groups as a function of VDF conversion, monitored by ^{19}F NMR spectroscopy (**Figures S7**, **S8**) are very different from those observed in RAFT[6b] and ITP.[18] The -CH_2CF_2-TEMPO chain end proportion initially decreases, but subsequently stabilizes at 77% after 20% conversion. Conversely, the proportion of -CF_2CH_2-TEMPO chain end stabilizes at around 23% after 20% conversion. NMR monitoring also reveals that the proportions of intrachain TT and HH reverse additions [**Eq. (S4)**, **(S5)**], which remain close to each other as expected,[6b] increase gradually with VDF conversion (**Figure S9**), reaching a plateau at ca. 4%. After an initial evolution phase, the fact that the polymerization continues at approximately the same rate with increasing molar masses, while the percentages of terminal HH and TT inversions no longer change, demonstrate that both types of dormant chains, PVDF-$CH_2CF_2Co^{III}$(acac)$_2$ and PVDF-CF_2CH_2-Co^{III}(acac)$_2$, are reactivated. Based on this study, we propose that the polymerization mechanism is that of a typical RDRP by reversible termination with Co^{II}(acac)$_2$ as the radical trapping species (**Scheme 1**).

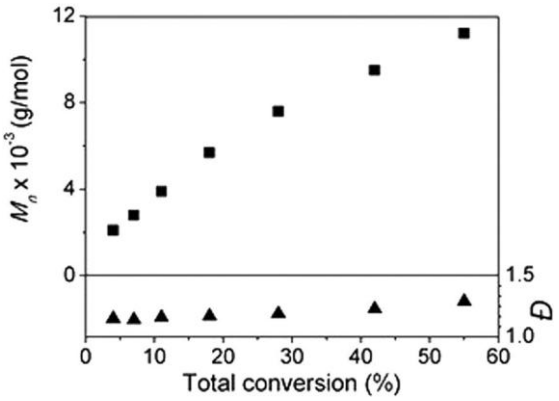

Figure 1. Plots of M_n (■) and $Đ$ (▲) versus conversion for the OMRP of VDF initiated by $R_0(VAc)_{\approx 4}Co(acac)_2$ at 4°8C in DMC (**Table S2**). $[VDF]_0/[R\text{-}Co]_0$=200.

Published in : Angewandte Chemie (2018), vol. 57, n°11, pp. 2934–2937
DOI: 10.1002/anie.201712347
Status : Postprint (Author's version)

The aptitude of both dormant species to reactivate may be evaluated from the results of a recent DFT study of the Co-C homolytic bond dissociation enthalpies (BDE) in various $(C_2H_{5-n}F_n)Co(acaca)_2$ molecules, with all possible F substitutions at the α and β positions.[19] The CH_3CF_2-$Co^{III}(acac)_2$ and CHF_2CH_2-$Co^{III}(acac)_2$ compounds which may be considered as models of the head and tail dormant chains, yield BDE_H = 27.4 kcalmol^{-1} {for CH_3CF_2-$Co^{III}(acac)_2$} and BDE_T = 26.0 kcalmol^{-1} {for HCF_2CH_2-$Co^{III}(acac)_2$}, respectively,[19] for a relative BDE difference of 1.4 kcalmol^{-1}, which is a very small number. Even more strikingly, the tail chain-end yields a weaker bond than the head chain-end, predicting an easier reactivation of the tail dormant species. In the case of the CH_3CF_2-X and CHF_2CH_2-X models of the "head" and "tail" dormant species in ITP (X=I) and RAFT {X=SC(S)OMe}, the BDE is greater for RAFT {ΔBDE= BDE_T-BDE_H =4.2 kcalmol^{-1} for I or 6.2 kcalmol^{-1} for SC(S)OMe.[8,19] To further improve the model, the chain simplification was implemented only at the level of the δC atom. Thus, PVDF-CF_2CH_2-$Co^{III}(acac)_2$ was modeled by $CHF_2CF_2CH_2$-$Co^{III}(acac)_2$, for which the calculated BDE is 25.2 kcalmol^{-1}, and PVDF-CH_2CF_2-$Co^{III}(acac)_2$ was modeled by $CHF_2CH_2CF_2$-$Co^{III}(acac)_2$ (product of a regular HT addition, BDE=27.9 kcalmol^{-1}) and $CH_3CH_2CF_2$-$Co^{III}(acac)_2$ (product of a TT addition, BDE=27.4 kcalmol^{-1}). For the computational details, see the **SI**. Qualitatively, the bond strengths remain in the order $PVDF_T$-$Co^{III}(acac)_2$ < $PVDF_H$-$Co^{III}(acac)_2$, predicting no accumulation of the $PVDF_T$-$Co^{III}(acac)_2$ in the medium (in contrast to what is observed in RAFT and ITP). In reality, the observation of a greater proportion of $PVDF_T$-$Co^{III}(acac)_2$ dormant chains (**Figure S8**) relative to the in-chain errors means that the experimental bond strengths must be in the opposite order ($PVDF_T$-$Co^{III}(acac)_2$ >$PVDF_H$-$Co^{III}(acac)_2$), but the difference must be much smaller than in the corresponding ITP and RAFT dormant species.

In addition to improved control in VDF homopolymerization, the labile carbon–metal bond in PVDF-$Co^{III}(acac)_2$ allowed reactivation for chain extension with VAc, leading to the preparation of PVDF-*b*-PVAc diblock copolymers increasing the scope of available PVDF-containing block copolymers.[6c,20] The SEC chromatograms (**Figure 2**A) a shift of the PVDF-$Co^{III}(acac)_2$ distribution (trace a, M_n=4100 g/ mol, $Đ$=1.27) toward higher molar masses upon chain extension to form the PVDF-*b*-PVAc diblock, while maintaining low $Đ$ values (trace b, M_n=10300 gmol^{-1}, $Đ$=1.28). As expected, the RI-SEC chromatograms of the PVDFs were negative (fluoropolymers have a low refractive index).[1b,7,21] ^{1}H and ^{19}F NMR spectra (**Figure S10** and **Figure 2**B, respectively) confirmed the structure of the product: characteristic -CH(OAc)- signal of PVAc at 4.8 ppm and the VDF-VAc dyad -CF_2- signal at -93.3 ppm, confirming the product structure.[6c]

Published in : Angewandte Chemie (2018), vol. 57, n°11, pp. 2934–2937
DOI: 10.1002/anie.201712347
Status : Postprint (Author's version)

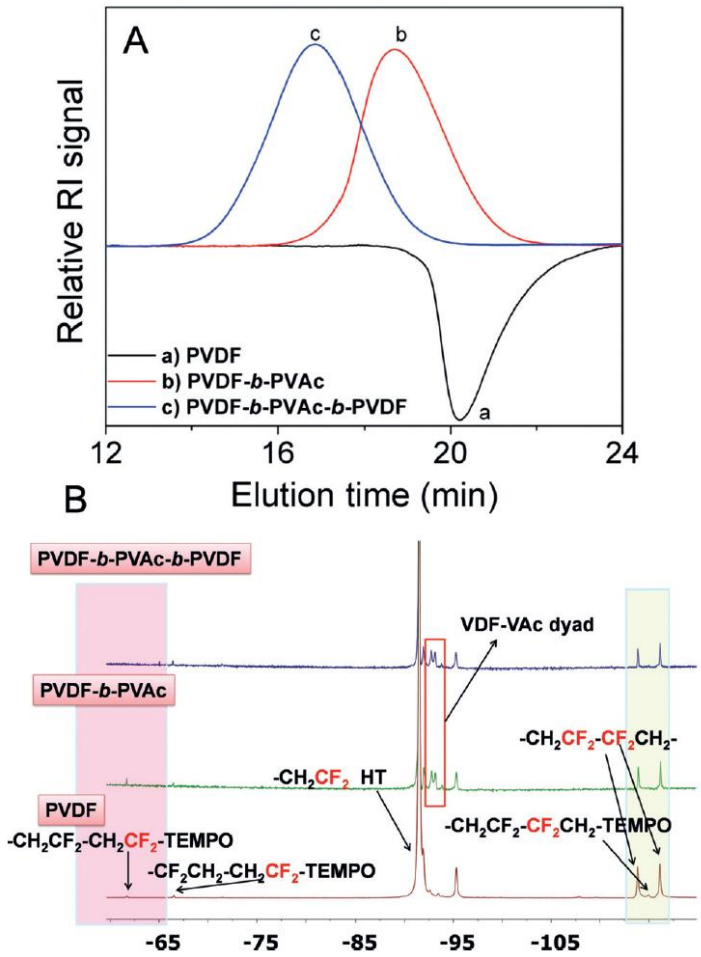

Figure 2. A) SEC traces of the PVDF prepared by $Co(acac)_2$-mediated OMRP (trace a, after 24 h), of the PVDF-*b*-PVAc diblock copolymer (trace b, after 24+24 h) obtained by chain extension with VAc, and of the PVDF-*b*-PVAc-*b*-PVDF triblock copolymer (trace c, after 24+24+16 h) prepared by chain coupling of the previous diblock copolymer using isoprene. B) ^{19}F NMR spectra of PVDF (bottom), of the PVDF-*b*-PVAc diblock copolymer (middle), and of the PVDF-*b*-PVAc-*b*-PVDF triblock copolymer (top).

$Co^{III}(acac)_2$-terminated polymers prepared by OMRP are known to undergo rapid chain–chain coupling upon addition of a conjugated diene,[22] affording double-molecular weight terminated products[22] and allowing the facile synthesis of symmetric ABA triblock copolymers when starting from $Co^{III}(acac)_2$-terminated on AB diblock copolymers. Application of this technique to PVDF-b-PVAc, using isoprene as coupling agent yielded a symmetrical PVDF-*b*-PVAc-*b*-PVDF triblock copolymer (**Scheme S1**). The SEC chromatograms revealed that the M_n of the coupled product approximately doubled (M_n =19900 $gmol^{-1}$ vs. 10300 $gmol^{-1}$) while the dispersity remained low ($Đ$=1.31, **Table S3**).

As expected, the thermal stability of the produced PVDFs increases with increasing $\mathbf{M_n}$ (P1–P3, **Table S1**), as shown by the thermogravimetric analyses (TGA; **Figure S11**). The melting points (T_m) of these samples, determined by differential scanning calorimetry, were similar (ca. 163°C; **Figure S12**). Expectedly, the degree of crystallinity increased from 34 to 54% (calculated using **Equation S3**) with increasing M_n.

The thermal stabilities (TGA, **Figure S13**) of the PVAc-containing di-/triblock copolymers were close to those of the PVDF homopolymers as evidenced by their $T_{d,10\%}$ decomposition temperatures (**Table S3**).

Published in : Angewandte Chemie (2018), vol. 57, n°11, pp. 2934–2937
DOI: 10.1002/anie.201712347
Status : Postprint (Author's version)

However, the di-and triblock copolymer displayed a T_g characteristic of the PVAc block (at ca. 35°C) and a reduced degree of crystallinity (≤80%) relative to neat PVDF (**Table S3**, **Figures S15**,**S16**).

In conclusion, we report the first example of an organometallic-mediated radical polymerization (OMRP) of VDF and demonstrate an unprecedented level of control for this monomer, including the first synthesis of a block copolymer with successful transition to a second RDRP process. This was possible thanks to the facile reactivation of the dormant species formed after an inverted monomer addition, $PVDF_T$-X, when X=$Co^{III}(acac)_2$, whereas the reactivation of these chains is inefficient in ITP (X=I) and RAFT (X=xanthate). As a result of the remarkable properties of the fluorinated groups (low dielectric constant and interesting thermal, electroactive and surface properties), the resulting copolymers might find applications in high value added materials (e.g., coatings, binders for lithium ion batteries, piezoelectric devices, and membranes).

Supporting Information

1. MATERIALS

All reagents were used as received unless described otherwise. 1,1Difluoroethylene (vinylidene fluoride, VDF) was kindly supplied by Solvay S.A. (Tavaux, France and Brussels, Belgium). Vinyl acetate (VAc, ≥99%, Aldrich) was stored under nitrogen and purged for 30 mins with nitrogen before use. Cobalt(II) acetylacetonate ($Co(acac)_2$, 97%, Aldrich) was stored under argon and used as received. 2,2,6,6-Tetramethylpiperidine 1-oxy (TEMPO, 98%, Aldrich) was used as received. 2,2′-Azobis(4-methoxy-2,4-dimethylvaleronitrile) (V-70, Wako) was stored at -20 °C and used as received. The organocobalt(III) adduct (R-Co) initiator [$Co(acac)_2(CH(OCOCH_3)CH_2)_{<4}$-$R_0$)], where R_0 is the primary radical generated by V-70, was prepared as described previously[1] and stored as a CH_2Cl_2 solution (0.14 M) at -20 °C under argon.

Dimethyl carbonate (DMC, 99%, Sigma-Aldrich) and chloroform ($CHCl_3$, ≥99%, SigmaAldrich) were degassed by purging with nitrogen for 30 mins before use. Acetone, and laboratory reagent grade pentane (purity >95%) were purchased from Sigma-Aldrich and used as received. Deuterated acetone (acetone-d_6) (purity>99.8%) used for NMR spectroscopy was purchased from Euroiso-top (Grenoble, France).

2. EXPERIMENTAL PROCEDURES

2.1. REPRESENTATIVE PROCEDURE FOR THE OMRP OF VDF MEDIATED BY R-CO

A typical homopolymerization of VDF (**P2**, **Table S1**) was performed in a 50-mL Hastelloy autoclave Parr system (HC 276) equipped with a manometer, a mechanical Hastelloy anchor, a rupture disk (3000 PSI), and inlet and outlet valves. An electronic device regulated and controlled both stirring and heating of the autoclave. Prior to reaction, the autoclave was pressurized with 30 bars of nitrogen for 1 h to check for leaks. The autoclave was then conditioned for the reaction with several nitrogen/vacuum cycles (10^{-2} mbar) to remove any trace of oxygen. A solution of organocobalt initiator (1.0 ml, 0.14 M

Published in : Angewandte Chemie (2018), vol. 57, n°11, pp. 2934–2937
DOI: 10.1002/anie.201712347
Status : Postprint (Author's version)

stock solution in CH_2Cl_2, 1.4×10^{-4} mol) was introduced under argon in a Schlenk tube and evaporated to dryness at room temperature under reduced pressure. Then 30 mL, previously nitrogen purged DMC was added to the Schlenk tube under argon. After this, the solution was transferred into the autoclave under vacuum using a cannula. The vessel was cooled in an acetone/liquid nitrogen bath to -115 °C and 3 freeze-pump-thaw cycles were applied before the VDF (2.0 g, 0.03 mol) was transferred into the autoclave under weight control. Then, after warming up to room temperature, the reactor was stirred and gradually heated up to 40 °C and the evolutions of pressure and temperature were recorded.

After 24 h, a degassed solution of TEMPO (130 mg, 8.4×10^{-4} mol, 6 equivalents with respect to R-Co) in THF (5 mL) was introduced in the reactor using a HPLC pump and left to react for 1 h at 40 °C to eliminate the cobalt complex from the end of the polymer chain, according to a previously reported procedure.[2] After 1 h, the autoclave was cooled to room temperature, and then placed in an ice bath. The unreacted VDF was purged off, the solvent was completely removed under vacuum. The total product mixture was precipitated from chilled pentane, filtered off and then dried under vacuum (20×10^{-3} bar, 50 °C) for 16 h. The yield of the polymerization was determined gravimetrically (mass of polymers obtained, 1.1 g / mass of monomer transferred into the pressure reactor, 2.0 g) (yield = 55%). The obtained PVDF, as a light brown color fine powder was characterized by ^{1}H and ^{19}F NMR spectroscopies. The product was analyzed by SEC in DMF (PMMA calibration to determine the molecular parameters of the polymer (molar mass and molar-mass distribution). The same experimental procedure (except the initial ratio of VDF to R-Co) was used for the other polymerizations. The results are summarized in **Table S1**, **P1-P3**.

^{1}H NMR (acetone-d_6) δ (ppm) (**Figure S2, P2, Table 1**): 0.80 to 1.40 (CH_3 and $-CH_2$ of TEMPO fragment at the ω-chain end and $-CH_3$ and $-CH_2$ of V-70 fragment at the α-chain end); 1.70 to 2.10 ($-OCOCH_3$ and $-CH_2$ of VAc oligomer); 2.10 to 2.40 (m, $-CF_2CH_2-CH_2CF_2-$ reverse T-T VDFVDF dyad addition); 2.45 to 3.10 (m, $-CH_2CF_2-CH_2CF_2-$, normal H-T VDF-VDF dyad addition), and a small triplet of triplets corresponding to the $-CH_2CF_2-H$ end-group caused either by the transfer to the solvent or polymer or from the backbiting (in the range of 6.05 to 6.45 ppm, $^{2}J_{HF}$ = 55 Hz, $^{3}J_{HH}$ = 4.6 Hz).

$$DP_n\ of\ VDF = \frac{\{\int_{2.70}^{3.15} CH_2\ (HT) + \int_{2.25}^{2.45} CH_2\ (TT)\}/2}{\int_{5.05}^{5.45} CH} \qquad (S1)$$

$$M_{n,NMR} = M_{R\text{-}Co} + \{M_{VDF} \times (\mathrm{DP}_n \text{ of VDF})\} \qquad (S2)$$

^{19}F NMR (acetone-d_6) δ (ppm) (**Figure S3**, **P2**, **Table 1**): -61.5 ($-CH_2CF_2-CH_2CF_2$-TEMPO); -66.5 ($-CF_2CH_2-CH_2CF_2$-TEMPO); -91.0 ($-CH_2CF_2-CH_2CF_2-$, normal VDF-VDF HT addition); -91.50 ($-CF_2CH_2-CH_2CF_2-CH_2CF_2-CH_2CF_2-$, normal VDF-VDF HT addition); -92.14 ($-CH_2CF_2CH_2CF_2$-H); -92.96 (oligo(VAc)- CH_2CF_2-PVDF); -94.78 ($-CF_2CH_2-CH_2CF_2-CH_2CF_2-$, TT (tailto-tail) reverse addition); -107.9 ($-CH_2CF_2-CF_2CH_3$); -113.8 ($-CH_2CF_2-CF_2CH_2$-TEMPO); -113.23 and -115.66 ($-CH_2CF_2-CH_2CF_2-CF_2CH_2-CH_2CF_2-CH_2CF_2-$, $-CH_2CF_2-CH_2CF_2-CF_2CH_2CH_2CF_2-CH_2CF_2-$, respectively, reverse H-H VDF-VDF dyad addition). -114.39 ($-CH_2CF_2CH_2CF_2-CH_2CF_2$-H and $-CF_2CH_2-CH_2CF_2-CH_2CF_2$-H).

^{13}C NMR (acetone-d_6) δ (ppm) (**Figure S4**, **P2**, **Table 1**): 21.45 {$-OCOCH_3$ of the α-chain end containing oligo(VAc)}; 40.30 {$-CH_2CH(OCOCH_3)$ of the α-chain end containing oligo(VAc)}; 44.30 ($-CH_2$ of VDF);

Published in : Angewandte Chemie (2018), vol. 57, n°11, pp. 2934–2937
DOI: 10.1002/anie.201712347
Status : Postprint (Author's version)

67.60 {-CH_2CH(OCOCH_3) of the α-chain end containing oligo(VAc)}; 117.8 to 123.90 (-CF_2 of VDF); 171.10 {-CH_2CH(OCOCH_3) of the α-chain end containing oligo(VAc)}.

2.2. KINETICS STUDY OF OMRP OF VDF MEDIATED BY R-CO.

A series of experiments were carried out for the OMRP of VDF mediated by R-Co and they were stopped at different polymerization times (0.5 h to 24 h) to monitor (i) the conversion of VDF by gravimetry and (ii) the evolution of the molar masses with time by means of SEC in DMF. The data is summarized in **Table S2**.

2.3. SYNTHESIS OF VDF-CONTAINING DIBLOCK- AND SYMMETRICAL TRIBLOCK-LIKE COPOLYMERS.

OMRP of VDF mediated by R-Co ($[VDF]_0$:$[R\text{-}Co]_0$ = 100) at 40 °C was set up using the procedure described above. After 24 h of reaction, an aliquot was picked out the medium into a nitrogen purged TEMPO solution in THF (to eliminate the cobalt complex from the copolymer chain-end and avoid undesired termination by bimolecular coupling)[2a] to determine the polymer composition (after removing of unreacted VDF at room temperature) by ^{1}H and ^{19}F NMR spectroscopy in acetone-d_6 and the molecular parameters by SEC in THF. Then unreacted VDF was purged off, VAc (10 mL, 108 mmol) was transferred in the reactor using an HPLC pump and the reaction was continued for another 24 h at 40 °C. After 24 h of reaction, an aliquot was picked out the medium and quenched with TEMPO to determine the polymer composition (after removing of unreacted VAc at room temperature) by ^{1}H and ^{19}F NMR spectroscopies in acetone-d_6 and the molecular parameters by SEC in THF. Then a degassed solution of isoprene (2 mL, 0.02 mol) in CH_2Cl_2 (5 mL) was introduced in the reactor under argon and left to react for 16 h at 40 °C. The reaction was stopped after 16 h and the autoclave was cooled to room temperature and then placed in an ice bath. After opening the vessel, the crude product was then dissolved in THF and precipitated from chilled pentane. It was then filtered and dried under vacuum (20×10^{-3} bar, 40 °C) for 16 h. The molecular parameters of the copolymer were measured by SEC in DMF using PMMA as calibration and the composition of the copolymer was determined by ^{1}H and ^{19}F NMR spectroscopies in acetone-d_6. The results are summarized in **Table S1**.

2.4 COMPUTATIONAL DETAILS.

The computational work was carried out using the Gaussian09 suite of programs.[3] The geometry optimizations were performed without any symmetry constraint using the BPW91* functional, a modified version of the B3PW91 functional, in which the c3 coefficient in Becke's original three-parameter fit to thermochemical data was changed to 0.15.[4] This specific functional was selected because it has proven more suited to the investigation of metal-containing systems where the spin state changes during the reaction.[5] In the present case, the dormant species (diamagnetic) yields a free radical (S = 1/2) and $Co^{II}(acac)_2$ (S = 3/2), for an overall spin S = 1 or 2.[6] The 6-31G(d,p) basis functions were used for the light atoms (H, C, F) whereas the Co and I atoms were treated with the LANL2DZ function augmented by an f polarization function (α = 2.78 for Co[7] and 0.289 for I[8]). The unrestricted formulation was used for open-shell molecules, yielding only minor spin contamination ($\langle S^2 \rangle$ at convergence was very close to the expected value of 0.75 for the radical species and 3.75 for the spin quartet species). All final geometries were characterized as local minima by verifying that all

Published in : Angewandte Chemie (2018), vol. 57, n°11, pp. 2934–2937
DOI: 10.1002/anie.201712347
Status : Postprint (Author's version)

second derivatives of the energy were positive. Thermochemical corrections were obtained at 298.15 K on the basis of frequency calculations, using the standard approximations (ideal gas, rigid rotor and harmonic oscillator). Corrections for dispersion were carried out at the fixed BPW91* optimized geometries using Grimme's D3 empirical method (BPW91*-D3), using SR6 and S8 parameters identical to those optimized for B3PW91.[9]

3. CHARACTERIZATION.

Size Exclusion Chromatography (SEC) Measurements. Molar masses (M_ns) and dispersities (*Đ*s) of the (co)polymers were determined by size exclusion chromatography (SEC) with a Agilent Technologies' triple-detection GPC (thermostated at 35 °C) using a PL0390-0605390 LC light scattering detector with two diffusion angles (15° and 90°), a PL0390-06034 capillary viscometer, and a 390-LC PL0390-0601 refractive index detector and two PL1113-6300 ResiPore 300 × 7.5 mm columns. Toluene was used as the flow rate marker, while DMF (containing 0.1 wt% of LiCl) was used as the eluent at a flow rate of 0.8 mL min^{-1}. Poly(methyl methacrylate) (PMMA) standards were used for the calibration and the results were processed using the corresponding Agilent software. Typical sample concentration used was 10 mg mL^{-1}.

Nuclear Magnetic Resonance (NMR) Spectroscopy. The compositions of the synthesized polymers and their microstructures were determined by ^{1}H, ^{13}C and ^{19}F NMR spectroscopies. ^{1}H, ^{13}C and ^{19}F 1D NMR spectra were recorded on a Bruker AC 400 Spectrometer (400 MHz for ^{1}H, 100 MHz for ^{13}C and 376 MHz for ^{19}F) using $CDCl_3$ or acetone-d_6 as a solvent using the following experimental conditions for ^{1}H [or ^{13}C or ^{19}F] NMR spectra: flip angle 90 ° [or 90 °or 30 °], acquisition time 4.5 s [or 0.3 s or 0.7 s], pulse delay 2 s [or 1 or 5 s], number of scans 32 [or 8192 or 64], and a pulse width of 12.5, 9.5, and 5.0 µs for ^{1}H ^{13}C and ^{19}F NMR, respectively. Coupling constants and chemical shifts are presented in Hertz (Hz) and parts per million (ppm), respectively. ^{1}H decoupling was realized with waltz16. ^{19}F decoupling was performed with nested loops using 0.5 ms and 1 ms chirped adiabatic pulses with 80 kHz band with in order to desynchronize and minimize decoupling artifacts.

Thermogravimetric Analysis (TGA). The purified and dried (co)polymer samples were subjected to TGA under air using a TGA 51 apparatus from TA Instruments at a heating rate of 10 °C min^{-1} from room temperature to 580 °C.

Differential Scanning Calorimetry (DSC). DSC analyses of the (co)polymer samples were performed under N_2 atmosphere using a Netzsch DSC 200 F3 instrument, calibrated with noble metals and checked before analysis with an indium sample (Tm = 156 °C). The heating or cooling range was from -40 °C to 200 °C at a scanning rate of 10 °C min^{-1} and the T_g was recorded in the second heating cycle to remove the previous thermal history of the sample. T_g was measured by the inflection point in the heat capacity jump. Melting transitions were determined at the maximum of the enthalpy peaks and its area determined the melting enthalpy (ΔHm).

Published in : Angewandte Chemie (2018), vol. 57, n°11, pp. 2934–2937
DOI: 10.1002/anie.201712347
Status : Postprint (Author's version)

The degrees of crystallinity (χ_c) of the VDF-based (co)polymers were calculated from equation[10] (**S3**):

$$\chi_c\ (\%) = \frac{\Delta H_m}{\Delta H_c \emptyset_m} \times 100 \qquad (S3)$$

where ΔH_c (104.5 J g^{-1}), ϕ_m, and ΔH_m stand for the melting enthalpy of a 100% crystalline PVDF,[11] the weight fraction of PVDF in the (co)polymer, and the heat of fusion (determined by DSC in J g^{-1}); respectively of the sample under consideration.

4. SUPPLEMENTARY TABLES.

Table S1. Experimental conditions and Results of OMRP of VDF Mediated by R-Co at 40 °C.[a]

entry	$\frac{[VDF]_0}{[R\text{-}Co]_0}$	conv. (%)	$M_{n,theo}$[b] (g/mol)	$M_{n,NMR}$[c]	$M_{n,SEC}$[d] (g/mol)	$Đ$[d]	$T_{d,10\%}$[e]	T_m[f]	χ_c[f] (%)
P1	100	52	3800	4020	5900	1.30	257	156	34
P2	200	55	7200	7540	11200	1.29	299	163	45
P3	300	54	10500	11800	14500	1.32	310	162	54

Acronyms: VDF: vinylidene fluoride; DMC: dimethyl carbonate. [a]Conditions: Volume of solvent = 30 mL. [b]Calculated using the yield as conversion and the following equation: $M_{n,theo}$ = ([VDF]$_0$/[RCo]$_0$ × yield × M_{VDF}) + M_R + MTEMPO - 1. [c]Calculated using equation (**S2**). [d]Molar masses (M_n)s and dispersity values ($Đ$) were determined by SEC in DMF (containing 0.1 wt% LiCl), system was calibrated using poly(methyl methacrylate) standards. [e]Assessed by thermogravimetric analysis (TGA), under air at 10 °C/min. [f]Determined by differential scanning calorimetry (DSC) from equation (**S3**).

Table S2. Reaction Conditions and Results for the Kinetics Study of OMRP of VDF Mediated by R-Co at 40 °C.[a]

entry	time (h)	convn (%)	$M_{n,theo}$[b] (g/mol)	$M_{n,SEC}$[c] (g/mol)	$Đ$[c]
1	0.5	4	1150	2100	1.15
2	1	7	1500	2800	1.14
3	2	11	2050	3900	1.16
4	5	18	2950	5700	1.17
5	9	28	4200	7600	1.19
6	15	42	6000	9500	1.23
7	24	55	7700	11200	1.29

Acronyms: VDF: vinylidene fluoride; DMC: dimethyl carbonate. [a]Conditions: Volume of solvent = 30 mL. [VDF]$_0$/[R-Co]$_0$ = 200. [b]Calculated using the yield as conversion and the following equation: $M_{n,theo}$ = ([VDF]$_0$/[R-Co]$_0$ × yield × M_{VDF}) + M_R + M_{TEMPO} – 1. [c]Molar masses (M_n)s and dispersity values ($Đ$) were determined by SEC in DMF (containing 0.1 wt% LiCl), system was calibrated using poly(methyl methacrylate) standards.

Published in : Angewandte Chemie (2018), vol. 57, n°11, pp. 2934–2937
DOI: 10.1002/anie.201712347
Status : Postprint (Author's version)

Table S3. Reaction Conditions and Results for the Synthesis of AB diblock PVDF-*b*-PVAc and ABA triblock copolymers (PVDF-*b*-PVAc-*b*-PVDF) resulting from the chain extension of in situ generated PVDF-Co(acac)$_2$ by VAc, followed by coupling with isoprene.

entry	block	polymer	time (h)	$M_{n,SEC}$[d] (g/mol)	$Đ$[d]	$T_{d,10\%}$[e] (°C)	T_g[f] (°C)	T_m[f] (°C)	X_c[f] (%)
P4	first[a]	PVDF	24	4100	1.27	299	-	167	29
P5	chain extension[c]	PVDF-*b*-PVAc	24	10300	1.28	310	35	170	8
P6	coupling[c]	PVDF-*b*-PVAc-*b*-PVDF	16	19900	1.31	305	35	169	1.5

[a]First block synthesized by OMRP of VDF at 40 °C mediated by 1.4 ×·10^{-4} mol of R-Co ($[VDF]_0/[R\text{-}Co]_0$ = 100). [b]Second block synthesized by chain extension of in situ generated PVDF-Co(acac)$_2$ by VAc at 40 °C. [c]Coupling in the presence of 2 mL of isoprene . [d]Determined by SEC in DMF (containing 0.1 wt% LiCl), system was calibrated using poly(methyl methacrylate) standards. [e]Assessed by thermogravimetric analysis (TGA), under air; 10 °C/min. [f]Determined by differential scanning calorimetry (DSC) using equation (**S3**).

Table S4. Energies (in hartrees), Cartesian coordinates (in Å) and views of all geometry-optimized molecules.

Radicals

$CF_2CH_2CF_2H$

E = -514.977191392
E-D3 = -514.984605675
H-D3 = -514.915423

6	1.337198000	-0.282193000	0.369586000
6	-0.076232000	-0.566653000	0.755887000
1	-0.190775000	-1.643247000	0.924058000
1	-0.306787000	-0.047390000	1.692043000
9	1.703331000	1.001365000	0.392278000
9	1.725199000	-0.856210000	-0.781359000
6	-1.096828000	-0.135897000	-0.291536000
9	-1.029540000	1.211500000	-0.473630000
9	-2.348135000	-0.442994000	0.156489000
1	-0.944963000	-0.623861000	-1.263738000

$CF_2CH_2CH_3$

E = -316.66773032
E-D3 = -316.673453797
H-D3 = -316.590875

6	0.635586000	0.000285000	0.411689000
6	-0.821471000	0.001936000	0.740700000
1	-1.025426000	-0.878859000	1.361217000
1	-1.024143000	0.885891000	1.357161000
9	1.072991000	1.097184000	-0.229763000
9	1.070892000	-1.098804000	-0.227688000
6	-1.717203000	-0.000403000	-0.508165000
1	-1.524866000	0.884755000	-1.123503000
1	-2.775208000	0.001254000	-0.224432000
1	-1.526782000	-0.889376000	-1.118728000

Published in : Angewandte Chemie (2018), vol. 57, n°11, pp. 2934–2937
DOI: 10.1002/anie.201712347
Status : Postprint (Author's version)

$CH_2CF_2CF_2H$

E = -514.968029876
E-D3 = -514.975310202
H-D3 = -514.908764

6	-1.422554000	1.194356000	-0.305769000
6	-0.630087000	-0.018377000	-0.006374000
1	-2.474705000	1.086570000	-0.546081000
1	-0.995461000	2.173948000	-0.124132000
9	-0.632952000	-0.277901000	1.342467000
9	-1.178840000	-1.107259000	-0.626617000
6	0.834258000	0.063391000	-0.464099000
9	1.394301000	1.194049000	0.047028000
9	1.514921000	-1.007391000	0.002417000
1	0.903593000	0.089781000	-1.559989000

Complexes

$Co(acac)_2$

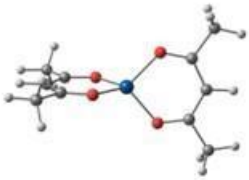

E = -835.694742101
E-D3 = -835.719573848
H-D3 = -835.4515291

27	0.000000000	-0.000068000	-0.000099000
6	3.396144000	1.774311000	1.773834000
6	2.560109000	0.886450000	0.886037000
6	3.198489000	0.000160000	-0.000003000
6	2.560280000	-0.886250000	-0.886038000
6	3.396481000	-1.774173000	-1.773616000
8	1.294510000	1.024212000	1.024059000
8	-1.294608000	1.024097000	-1.024208000
6	-2.560198000	0.886041000	-0.886348000
6	-3.396317000	1.773942000	-1.774025000
8	1.294703000	-1.024394000	-1.023927000
8	-1.294605000	-1.024155000	1.024130000
6	-2.560191000	-0.886220000	0.886167000
6	-3.396308000	-1.773792000	1.774175000
6	-3.198489000	-0.000064000	-0.000067000
1	3.143804000	1.576815000	2.822675000
1	4.469963000	1.629149000	1.628100000
1	3.143155000	2.823089000	1.576883000
1	4.284321000	0.000227000	0.000034000
1	3.143550000	-2.822950000	-1.576578000
1	4.470273000	-1.628915000	-1.627773000
1	3.144246000	-1.576811000	-2.822506000
1	-3.143404000	-2.822645000	1.577510000
1	-3.143961000	-1.576033000	2.822964000
1	-4.470113000	-1.628577000	1.628395000
1	-4.284321000	0.000009000	0.000009000
1	-3.143429000	2.822734000	-1.576992000
1	-4.470122000	1.628681000	-1.628285000
1	-3.143960000	1.576552000	-2.822877000

Published in : Angewandte Chemie (2018), vol. 57, n°11, pp. 2934–2937
DOI: 10.1002/anie.201712347
Status : Postprint (Author's version)

$Co(acac)_2(CF_2CH_2CF_2H)$

E = -1350.70258374
E-D3 = -1350.75291893
H-D3 = -1350.436217

27	-0.264645000	-0.742862000	0.302074000
8	-1.683524000	-1.334120000	-0.757643000
6	-2.911299000	-1.010451000	-0.618224000
6	-3.413476000	-0.169401000	0.384785000
6	-2.606354000	0.402043000	1.372976000
8	-1.337852000	0.246951000	1.470753000
6	-3.839773000	-1.615420000	-1.637617000
6	-3.214655000	1.270156000	2.443099000
8	1.085058000	-0.466148000	1.574192000
6	2.281721000	-0.924334000	1.530092000
6	2.787342000	-1.745611000	0.518649000
6	1.980909000	-2.254701000	-0.511686000
8	0.745912000	-1.980486000	-0.674161000
6	3.150170000	-0.523776000	2.693932000
6	2.552473000	-3.216277000	-1.519686000
6	0.099897000	0.786561000	-0.771869000
6	0.923505000	1.850984000	-0.067124000
1	-2.935626000	0.883870000	3.430262000
1	3.195829000	0.569807000	2.760174000
1	2.694903000	-0.881285000	3.625407000
1	-4.304105000	1.320379000	2.367518000
1	4.164201000	-0.924178000	2.612984000
1	-2.803592000	2.284306000	2.366991000
1	-4.478912000	0.035598000	0.403556000
1	3.824910000	-2.058953000	0.570925000
1	-3.689845000	-2.700448000	-1.671360000
1	3.580641000	-3.504793000	-1.285388000
1	-4.890012000	-1.397723000	-1.425763000
1	1.922218000	-4.111413000	-1.568384000
1	-3.584712000	-1.224540000	-2.630320000
1	2.526129000	-2.750223000	-2.512278000
1	1.946087000	1.490178000	0.073893000
9	0.701830000	0.406149000	-1.928845000
9	-1.103081000	1.343407000	-1.138475000
1	0.487053000	2.030360000	0.919504000
6	0.983817000	3.165071000	-0.822744000
1	-0.004889000	3.580208000	-1.056873000
9	1.659517000	4.075137000	-0.054871000
9	1.672035000	3.019473000	-1.989971000

$Co(acac)_2(CF_2CH_2CH_3)$

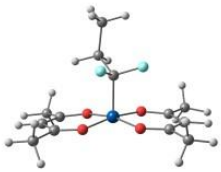

E = -1152.392611
E-D3 = -1152.44105605
H-D3 = -1152.110987

27	-0.011667000	0.217232000	-0.420606000
8	-1.285017000	1.542514000	-0.092672000
6	-2.549326000	1.417543000	-0.228720000

Published in : Angewandte Chemie (2018), vol. 57, n°11, pp. 2934–2937
DOI: 10.1002/anie.201712347
Status : Postprint (Author's version)

6	-3.200690000	0.264270000	-0.685816000
6	-2.516249000	-0.893497000	-1.070604000
8	-1.245603000	-1.043934000	-1.037917000
6	-3.344140000	2.641917000	0.142517000
6	-3.276321000	-2.091261000	-1.577970000
8	1.273432000	-0.966482000	-1.109117000
6	2.539674000	-0.781767000	-1.148567000
6	3.197918000	0.361997000	-0.684872000
6	2.506213000	1.494113000	-0.225435000
8	1.238787000	1.581329000	-0.117241000
6	3.321732000	-1.911934000	-1.766889000
6	3.260556000	2.739615000	0.161243000
6	-0.070441000	-0.446146000	1.369284000
6	0.669010000	-1.753015000	1.595304000
1	-2.853811000	-2.415578000	-2.535715000
1	3.118415000	-2.840840000	-1.220972000
1	2.981422000	-2.066285000	-2.797919000
1	-4.343063000	-1.885212000	-1.700631000
1	4.398286000	-1.720903000	-1.769129000
1	-3.152605000	-2.922534000	-0.872688000
1	-4.283516000	0.274446000	-0.757360000
1	4.280346000	0.404063000	-0.750579000
1	-2.943093000	3.513704000	-0.386710000
1	4.337294000	2.643919000	-0.003050000
1	-4.407834000	2.533066000	-0.086005000
1	2.878157000	3.590006000	-0.415045000
1	-3.225113000	2.834271000	1.215916000
1	3.073334000	2.959285000	1.219209000
1	1.730516000	-1.574686000	1.392970000
9	0.408166000	0.510949000	2.217374000
9	-1.390131000	-0.609158000	1.706213000
1	0.313937000	-2.471021000	0.848851000
6	0.478576000	-2.287077000	3.017867000
1	-0.576662000	-2.495204000	3.221902000
1	1.043504000	-3.216283000	3.153823000
1	0.831311000	-1.561571000	3.758728000

$Co(acac)_2(CH_2CF_2CF_2H)$

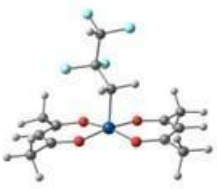

E = -1152.392611
E-D3 = -1152.44105605
H-D3 = -1152.110987

27	-0.287612000	0.889256000	0.216283000
8	-1.707826000	-1.492015000	-0.848844000
6	-2.931905000	-1.136004000	-0.735940000
6	-3.434474000	-0.300254000	0.269292000
6	-2.651020000	0.148027000	1.343655000
8	-1.399642000	-0.071292000	1.476078000
6	-3.854413000	-1.708783000	-1.780238000
6	-3.277155000	0.930189000	2.467873000
8	1.067690000	-0.579444000	1.453118000
6	2.280148000	-0.977316000	1.375503000
6	2.801948000	-1.762755000	0.339354000
6	2.025016000	-2.199034000	-0.737440000
8	0.782358000	-1.933667000	-0.904344000
6	3.160100000	-0.527000000	2.509694000
6	2.631081000	-3.060661000	-1.814476000
6	-0.150629000	0.682255000	-0.874412000

Published in : Angewandte Chemie (2018), vol. 57, n°11, pp. 2934–2937
DOI: 10.1002/anie.201712347
Status : Postprint (Author's version)

6	0.799723000	1.762061000	-0.449163000
1	-3.107826000	0.403776000	3.414602000
1	3.297729000	0.558696000	2.432065000
1	2.660694000	-0.722680000	3.464775000
1	-4.350613000	1.079816000	2.324516000
1	4.139139000	-1.013670000	2.497285000
1	-2.780504000	1.904166000	2.549876000
1	-4.491077000	-0.052971000	0.258953000
1	3.849009000	-2.045299000	0.375852000
1	-3.802264000	-2.803575000	-1.748692000
1	3.671890000	-3.319641000	-1.602487000
1	-4.891422000	-1.393476000	-1.637354000
1	2.041924000	-3.978682000	-1.922573000
1	-3.515293000	-1.400848000	-2.776471000
1	2.581110000	-2.532378000	-2.774441000
1	-1.165242000	1.092393000	-0.905092000
1	0.128695000	0.308270000	-1.865225000
9	0.550972000	2.212416000	0.810000000
9	2.106033000	1.331318000	-0.485249000
6	0.761979000	2.986861000	-1.385489000
9	-0.507009000	3.477582000	-1.439310000
9	1.573134000	3.955110000	-0.896693000
1	1.088387000	2.724013000	-2.401318000

5. SUPPLEMENTARY SCHEMES.

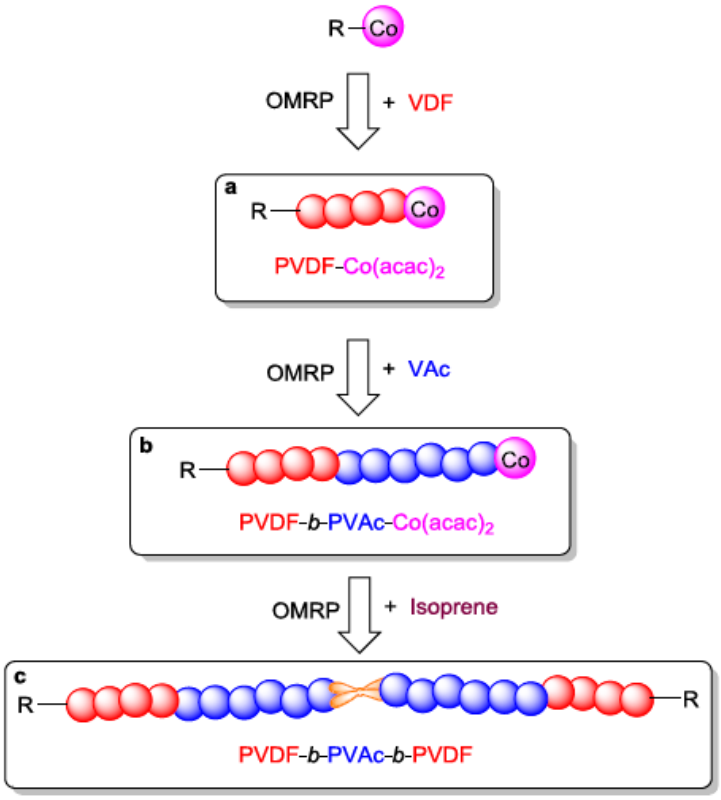

Scheme S1. Synthesis of PVDF and VDF-containing Diblock- and Symmetrical Triblock-like Copolymers via $Co(acac)_2$-mediated OMRP at 40 °C.

Published in : Angewandte Chemie (2018), vol. 57, n°11, pp. 2934–2937
DOI: 10.1002/anie.201712347
Status : Postprint (Author's version)

6. SUPPLEMENTARY FIGURES

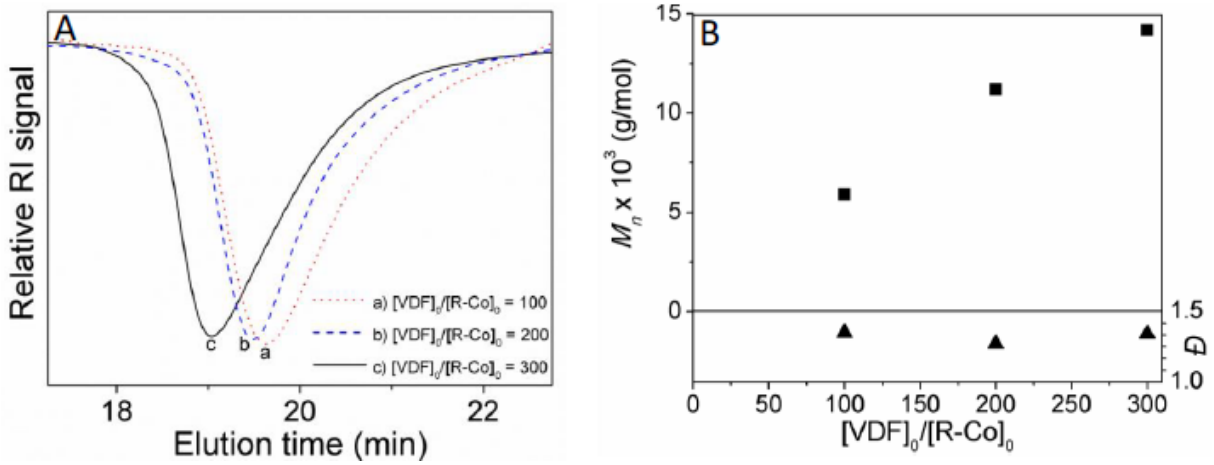

Figure S1. (A) Evolutions of the SEC traces vs initial $[VDF]_0$:$[R\text{-}Co]_0$ molar ratio and (B) plot of molar mass (M_n) and dispersity values ($Đ$) vs initial $[VDF]_0$:$[R\text{-}Co]_0$ molar ratio for the OMRP of VDF mediated by R-Co in DMC at 40 °C (**P1**-**P3**, **Table S1**). The conversion in each case is 50%.

The deviation of M_ns from theoretical M_ns might be due to the fact that poly(methyl methacrylate) samples (having different hydrodynamic diameter than that of PVDF) were used for the SEC calibration

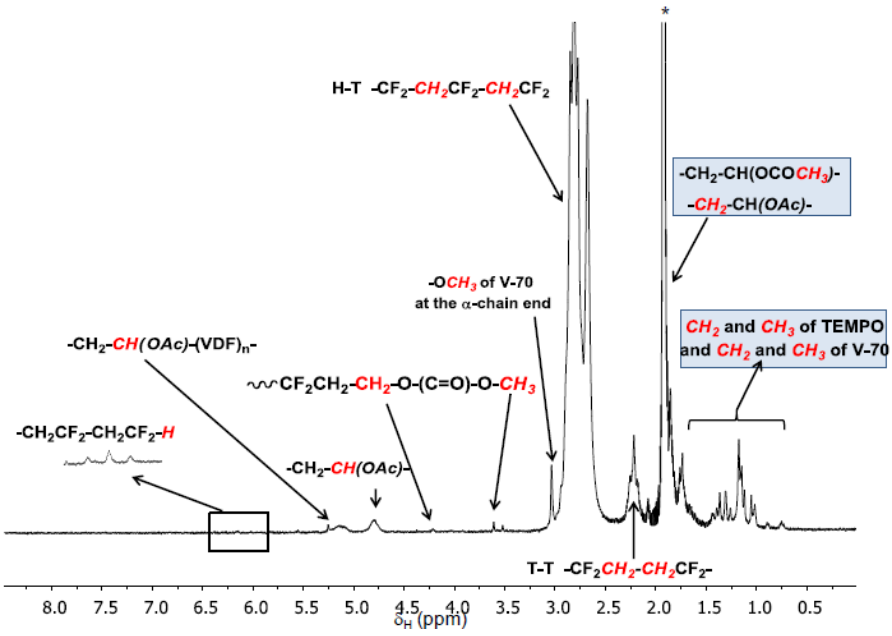

Figure S2. Representative ^{1}H NMR spectrum of PVDF (**P2**, **Table S1**) prepared by OMRP of VDF mediated by R-Co at 40 °C in DMC and quenched with TEMPO, recorded in acetone-d_6 at 20 °C. (*) Solvent (acetone) peak.

Published in : Angewandte Chemie (2018), vol. 57, n°11, pp. 2934–2937
DOI: 10.1002/anie.201712347
Status : Postprint (Author's version)

A typical ^{1}H NMR spectrum of the PVDF prepared by OMRP, after quenching with TEMPO (**Figure S2**, **P2**, **Table S1**), revealed: (i) signals corresponding to the oligo(VAc) from the R-Co; (ii) signals assigned to methylenes in PVDF block for both the normal head-to-tail (HT, major) and the inverted tail-to-tail (TT, minor) additions; and (iii) signals of the TEMPO chain ends. The spectrum also shows a small triplet of triplets for the -CH_2CF_2-H end-group caused by transfer to either solvent, monomer, polymer or from backbiting[12].

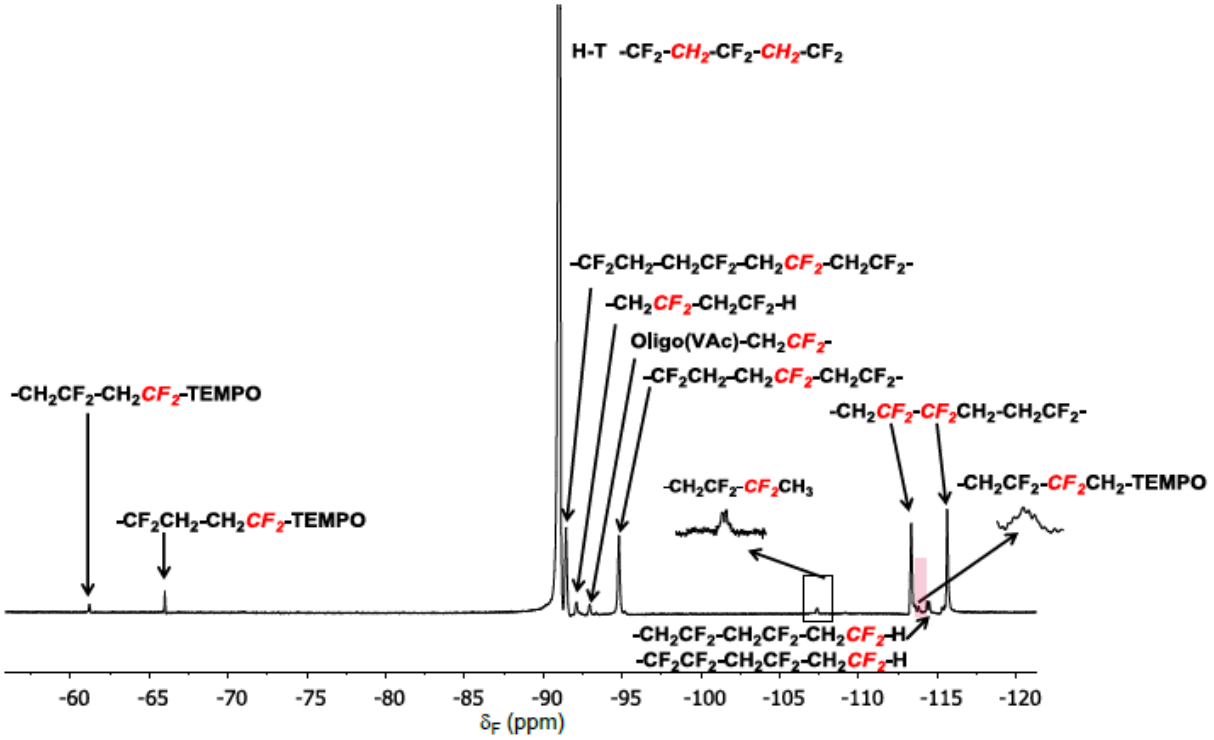

Figure S3. Representative ^{19}F NMR spectrum of PVDF (**P2**, **Table S1**) prepared by OMRP of VDF mediated by R-Co at 40 °C in DMC and quenched with TEMPO, recorded in acetone-d_6 at 20 °C.

The ^{19}F NMR spectrum (**Figure S3**) confirms the presence of the normal and inverted sequences,[13] as well as -C$\underline{F}_2$$CH_3$-terminated dead chains resulting from the chain transfer processes and irreversible transfer respectively.[14] The resonances of the VDF units at the α-chain end (R_0-(VAc)$_{\sim 4}$-$CH_2C\underline{F}_2$-, but notably not R_0-(VAc)$_{\sim 4}$-$CF_2C\underline{H}_2$- and ω-chain end (both -CF_2CH_2-$CH_2C\underline{F}_2$-TEMPO and -CH_2CF_2-$CH_2C\underline{F}_2$-TEMPO) have also been identified. The never reported signals centered at -61.5 and -66.5 ppm were assigned to –CF_2 groups adjacent to the TEMPO oxygen atom in CH_2CF_2-$CH_2C\underline{F}_2$-TEMPO and CF_2CH_2-$CH_2C\underline{F}_2$-TEMPO, respectively by analogy with those of difluoromethylenes in -$CF_2C\underline{F}_2O$-, R_F-$CH_2C\underline{F}_2$-I and R_F-$CF_2C\underline{F}_2$-I centered at -78 ppm,[15] -39, and -59 ppm, respectively.[16]

Published in : Angewandte Chemie (2018), vol. 57, n°11, pp. 2934–2937
DOI: 10.1002/anie.201712347
Status : Postprint (Author's version)

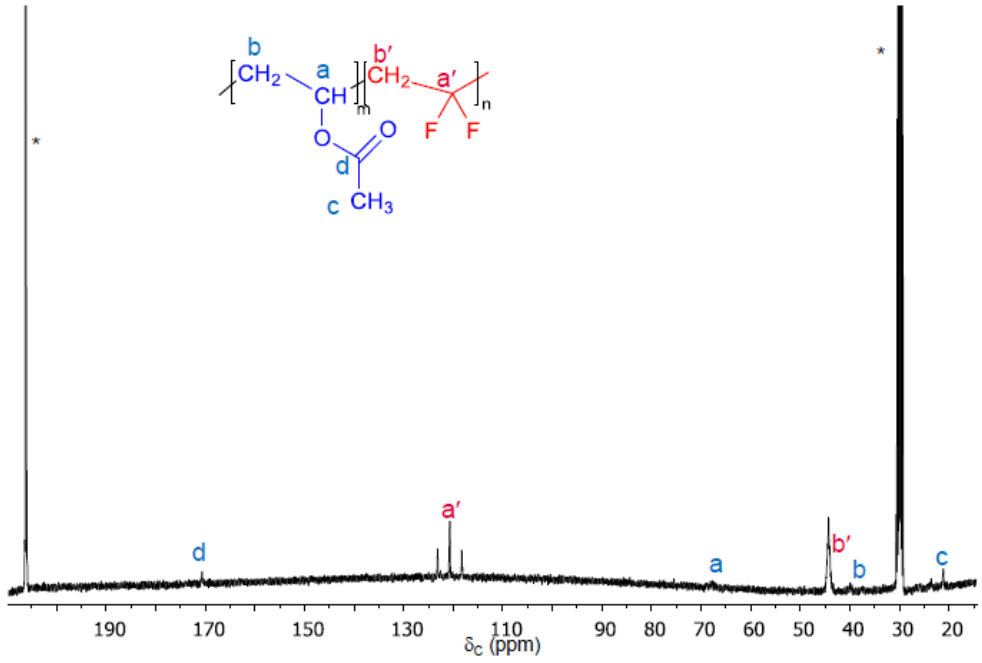

Figure S4. Representative ^{13}C NMR spectrum of PVDF (**P2**, **Table S1**) prepared by OMRP of VDF mediated by R-Co at 40 °C in DMC and quenched with TEMPO, recorded in acetone-d_6 at 20 °C. (*) Solvent (acetone) peak.

^{13}C NMR spectrum analysis (**Figure S4**) enabled the proper assignment of the position of all the carbon atoms in the PVDF homopolymer. It exhibits the characteristic signals at 21.45 {-OCO$\underline{C}H_3$ of the α-chain end containing oligo(VAc)}; 40.30 {-$\underline{C}H_2CH(OCO\underline{C}H_3)$ of the α-chain end containing oligo(VAc)}; 44.30 (-$\underline{C}H_2$ of VDF, triplet with $^2J_{CF}$= 32 Hz); 67.60 {$CH_2\underline{C}H(OCO\underline{C}H_3)$ of the α-chain end containing oligo(VAc)}; 117.8 to 123.90 (characteristic triplet with $^1J_{CF}$= 253 Hz), assigned to -$\underline{C}F_2$ of VDF); 171.10 {-$CH_2CH(O\underline{C}OCH_3)$ of the α-chain end containing oligo(VAc)}.

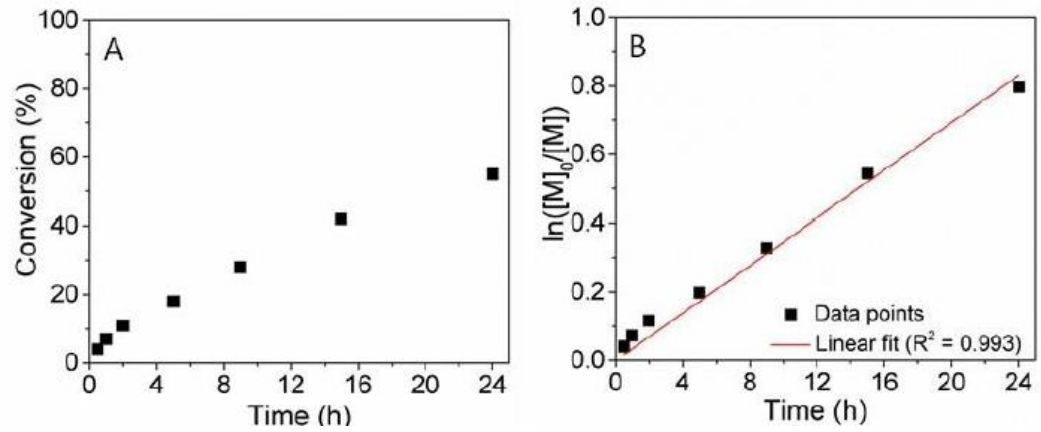

Figure S5. Conversion vs time (A) and ln$[M]_0$/[M] vs time (B) plots for the OMRP of VDF mediated by R-Co at 40 °C in DMC (entries 1-7, **Table S2**).

Published in : Angewandte Chemie (2018), vol. 57, n°11, pp. 2934–2937
DOI: 10.1002/anie.201712347
Status : Postprint (Author's version)

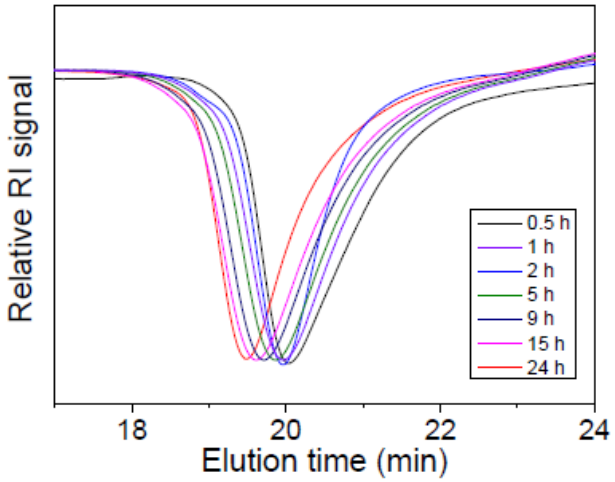

Figure S6. Evolution of the SEC traces vs time for the OMRP of VDF mediated by R-Co at 40 °C in DMC (entries 1-7, **Table S2**).

The deviation of M_ns from theoretical M_ns might be due to the fact that poly(methyl methacrylate) samples (having different hydrodynamic diameter than that of PVDF) were used for the SEC calibration.

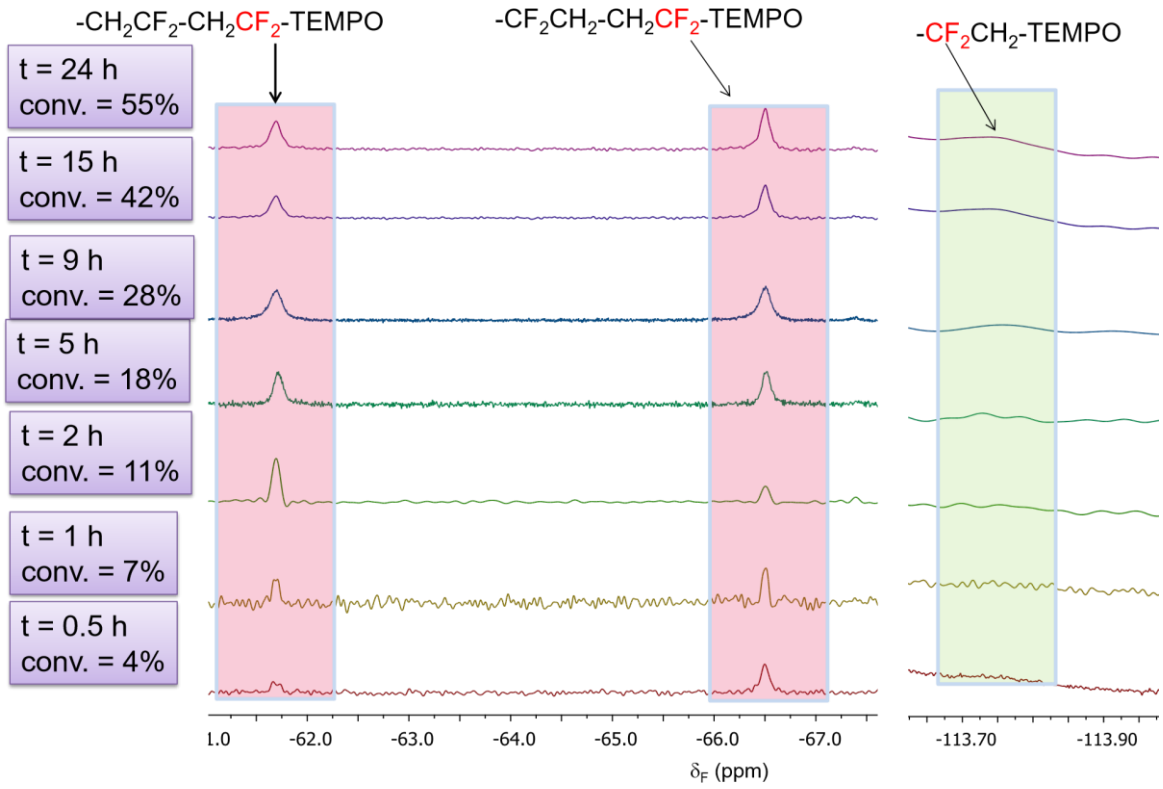

Figure S7. Evolutions of selected ^{19}F NMR signals with VDF conversion for PVDF homopolymers synthesized *via* OMRP. The spectra were recorded in acetone-d_6 at room temperature.

Published in : Angewandte Chemie (2018), vol. 57, n°11, pp. 2934–2937
DOI: 10.1002/anie.201712347
Status : Postprint (Author's version)

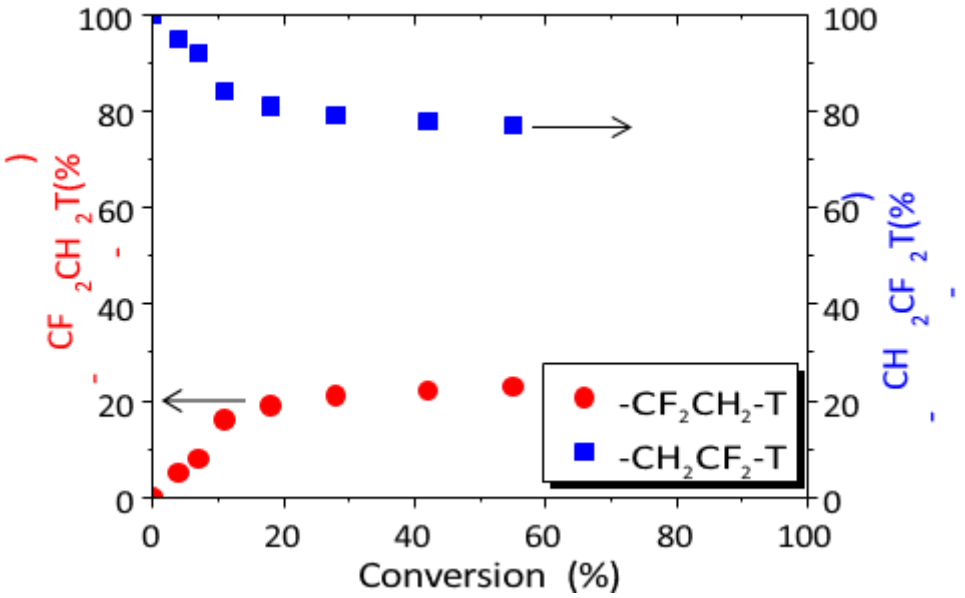

Figure S8. Evolutions of the chain-end functionalities for the OMRP of VDF mediated by R-Co at 40 °C in DMC after quenching by TEMPO. $[VDF]_0/[R\text{-}Co]_0$ = 200. "T" stands for TEMPO.

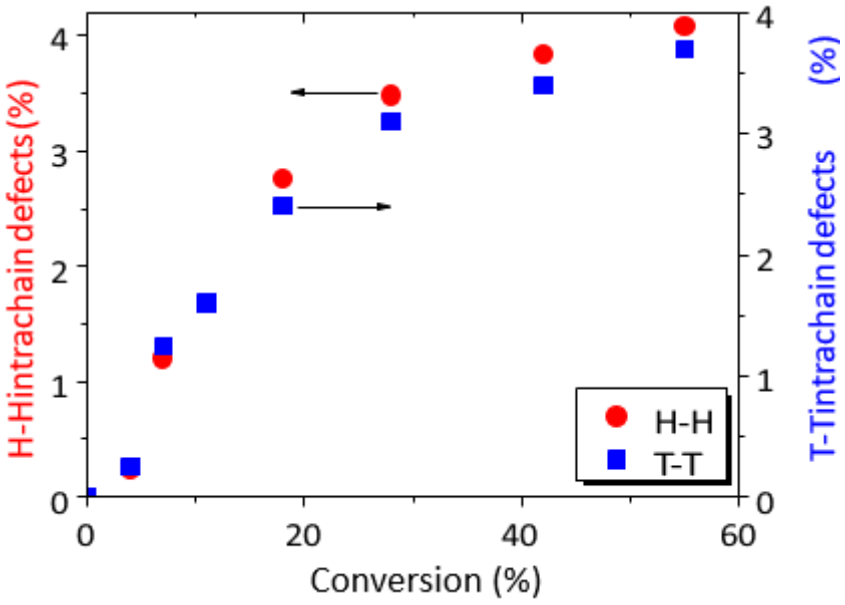

Figure S9. Evolutions of HH and TT intrachain additions vs. conversion during OMRP of VDF mediated by R-Co at 40 °C in DMC. $[VDF]_0/[R\text{-}Co]_0$ = 200

Published in : Angewandte Chemie (2018), vol. 57, n°11, pp. 2934–2937
DOI: 10.1002/anie.201712347
Status : Postprint (Author's version)

$$\%TT\ intra-chain = \frac{\int_{2.10}^{2.40} CH_2\ (TT)}{\int_{2.10}^{2.40} CH_2\ (TT) + \int_{2.45}^{3.10} CH_2\ (HT)} \qquad (S4)$$

$$\%HH\ intra-chain = \frac{\int_{-113.3}^{-114.5} CF_2\ (HH)}{\int_{-113.3}^{-114.5} CF_2\ (HH) + \int_{-88.5}^{-95.5} CF_2 + \int_{-115.5}^{-117.9} CF_2\ (HH)} \qquad (S5)$$

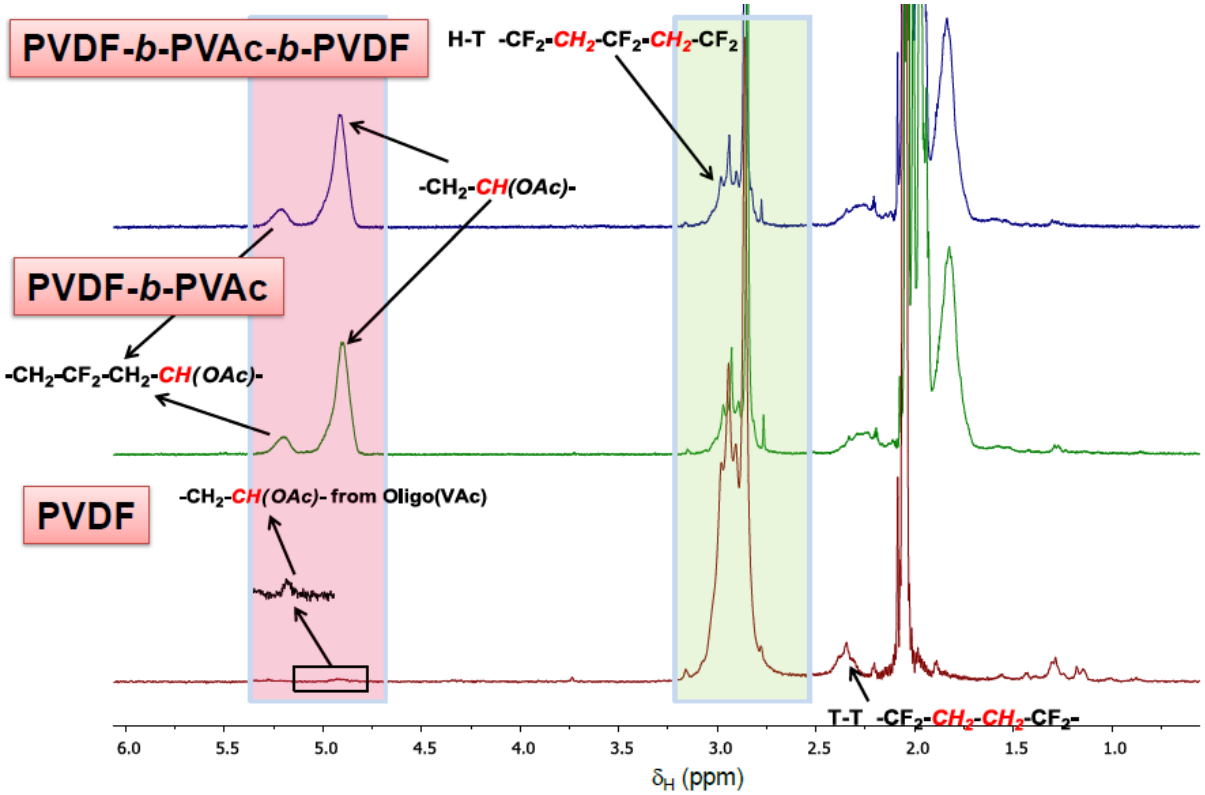

Figure S10. ^{1}H NMR spectra of PVDF (bottom), of the PVDF-*b*-PVAc diblock copolymer (middle), and of the PVDF-*b*-PVAc-*b*-PVDF triblock copolymer (top).

Published in : Angewandte Chemie (2018), vol. 57, n°11, pp. 2934–2937
DOI: 10.1002/anie.201712347
Status : Postprint (Author's version)

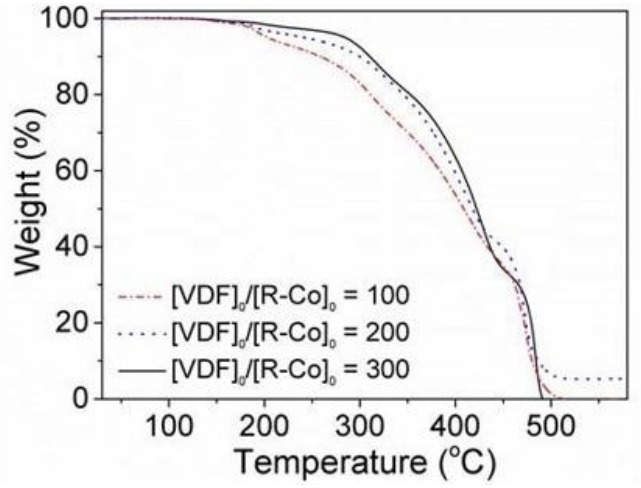

Figure S11. TGA thermograms (recorded under air) of PVDF samples (**P1**-**P3**, Table S1) prepared by OMRP of VDF mediated by R-Co at 40 °C in DMC using different initial $[VDF]_0$:$[R\text{-}Co]_0$ molar ratio.

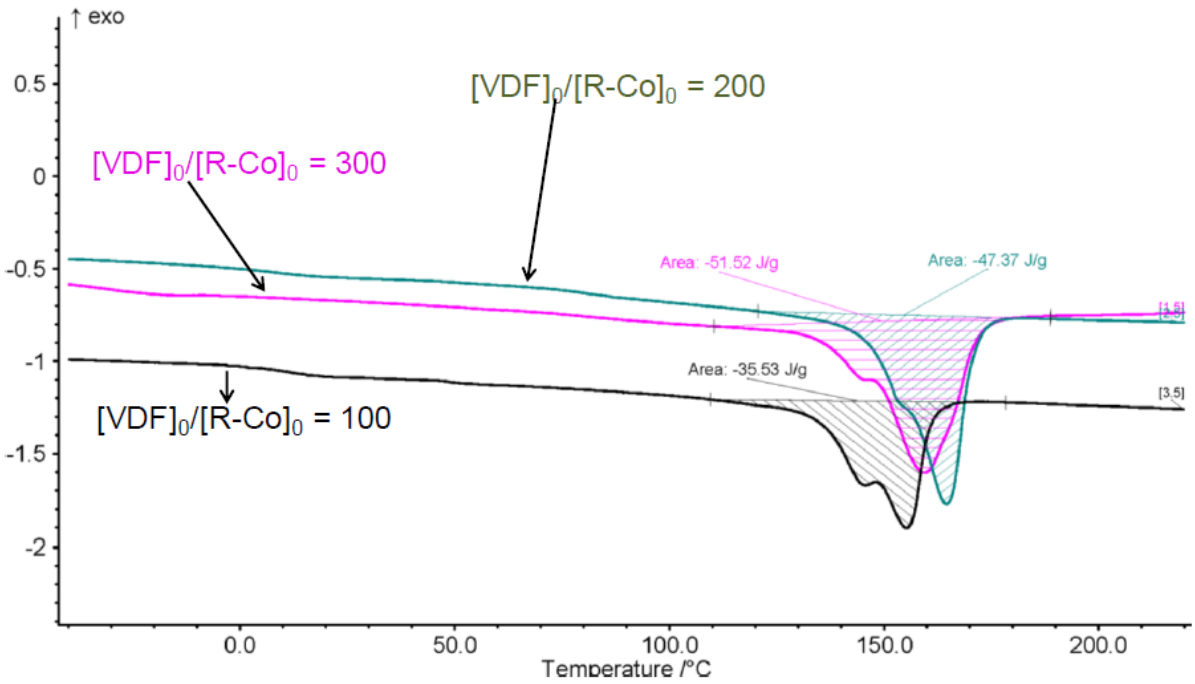

Figure S12. DSC thermograms of PVDFs (**P1-P3**, **Table S1**) prepared by OMRP of VDF mediated by R-Co at 40 °C in DMC using different initial $[VDF]_0$:$[R\text{-}Co]_0$ molar ratio.

Published in : Angewandte Chemie (2018), vol. 57, n°11, pp. 2934–2937
DOI: 10.1002/anie.201712347
Status : Postprint (Author's version)

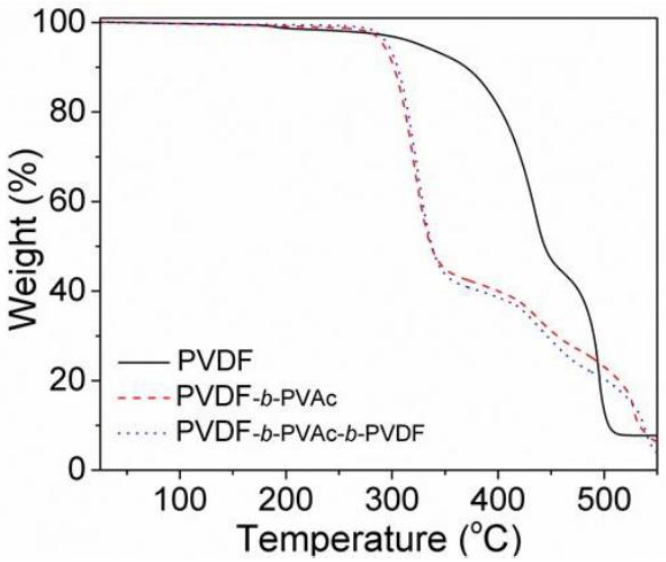

Figure S13. TGA thermograms (under air) of VDF-containing diblock-like and symmetrical triblock-like copolymers (**P4**-**P6**, **Table S3**) at 40 °C: the first PVDF block (a), chain extension with VAc to yield the PVDF-*b*-PVAc diblock copolymer (b), and addition of isoprene to couple the chains into the symmetrical PVDF-*b*-PVAc-*b*-PVDF triblock copolymer (c).

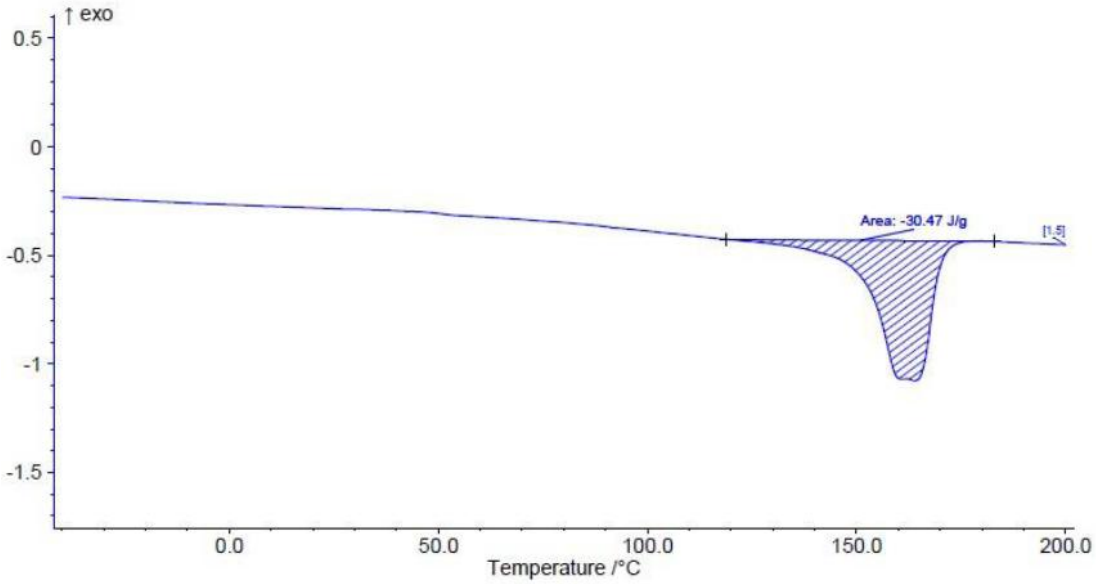

Figure S14. DSC thermograms of PVDF (**P4**, **Table S3**) by OMRP of VDF mediated by R-Co at 40 °C in DMC (after quenching with TEMPO).

Published in : Angewandte Chemie (2018), vol. 57, n°11, pp. 2934–2937
DOI: 10.1002/anie.201712347
Status : Postprint (Author's version)

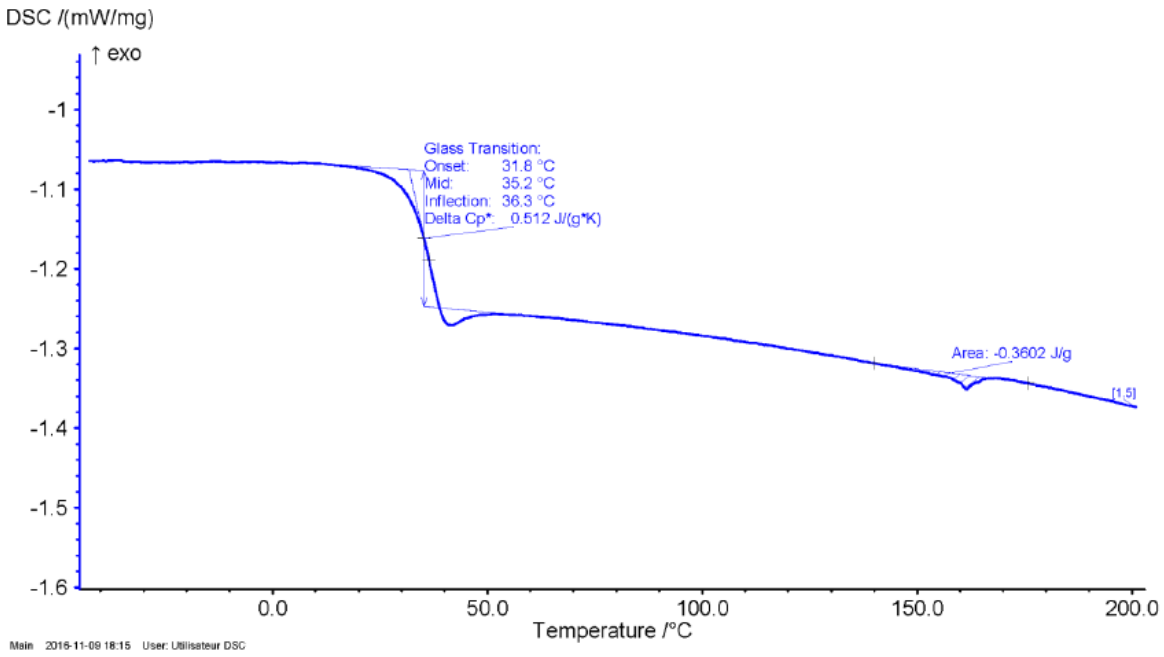

Figure S15. DSC thermogram of PVDF-*b*-PVAc diblock copolymer (**P5**, **Table S3**) prepared by chain extension with VAc from the in situ formed PVDF-Co(acac)$_2$ (and then quenched with TEMPO)

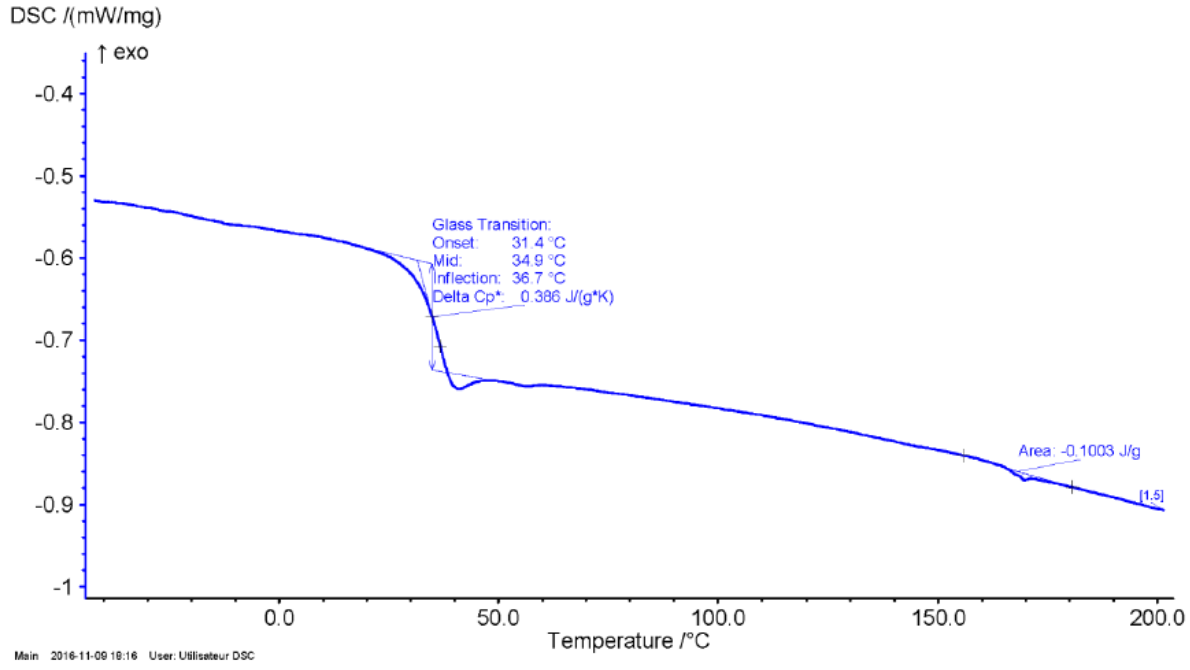

Figure S16. DSC thermogram of PVDF-*b*-PVAc-*b*-PVDF triblock copolymer (**P6**, **Table S3**) prepared by addition of isoprene to favor the *in situ* coupling of PVDF-*b*-PVAc-Co(acac)$_2$ chains.

Published in : Angewandte Chemie (2018), vol. 57, n°11, pp. 2934–2937
DOI: 10.1002/anie.201712347
Status : Postprint (Author's version)

7. REFERENCES

[1] Debuigne, Y. Champouret, R. Jerome, R. Poli, C. Detrembleur, *Chem. Eur. J.* **2008**, *14*, 4046-4059.
[2] a) A. Debuigne, J.-R. Caille, R. Jerome, *Macromolecules* **2005**, *38*, 5452-5458; b) A. N. Morin, C. Detrembleur, C. Jerome, P. De Tullio, R. Poli, A. Debuigne, *Macromolecules* **2013**, *46*, 4303-4312.
[3] M. J. Frisch, G. W. Trucks, H. B. Schlegel, G. E. Scuseria, J. R. C. M. A. Robb, G. Scalmani, V. Barone, B. Mennucci, G. A. Petersson, H. Nakatsuji, M. Caricato, X. Li, H. P. Hratchian, A. F. Izmaylov, J. Bloino, G. Zheng, J. L. Sonnenberg, M. Hada, M. Ehara, K. Toyota, R. Fukuda, J. Hasegawa, M. Ishida, T. Nakajima, Y. Honda, O. Kitao, H. Nakai, T. Vreven, J. A. Montgomery, Jr., J. E. Peralta, F. Ogliaro, M. Bearpark, J. J. Heyd, E. Brothers, K. N. Kudin, V. N. Staroverov, R. Kobayashi, J. Normand, K. Raghavachari, A. Rendell, J. C. Burant, S. S. Iyengar, J. Tomasi, M. Cossi, N. Rega, J. M. Millam, M. Klene, J. E. Knox, J. B. Cross, V. Bakken, C. Adamo, J. Jaramillo, R. Gomperts, R. E. Stratmann, O. Yazyev, A. J. Austin, R. Cammi, C. Pomelli, J. W. Ochterski, R. L. Martin, K. Morokuma, V. G. Zakrzewski, G. A. Voth, P. Salvador, J. J. Dannenberg, S. Dapprich, A. D. Daniels, O. Farkas, J. B. Foresman, J. V. Ortiz, J. Cioslowski, and D. J. Fox, Gaussian, Inc., Wallingford CT, **2009**.
[4] M. Reiher, *Inorg. Chem.* **2002**, *41*, 6928-6935.
[5] a) O. Salomon, M. Reiher, B. A. Hess, *J. Chem. Phys.* **2002**, *117*, 4729-4737; b) J. N. Harvey, R. Poli, *Dalton Trans.* **2003**, 4100-4106; c) J. N. Harvey, *Structure and Bonding* **2004**, *112*, 151 - 184; dJ.-L. Carreón-Macedo, J. N. Harvey, *J. Am. Chem. Soc.* **2004**, *126*, 5789-5797.
[6] a) A. Debuigne, C. Michaux, C. Jérôme, R. Jérôme, R. Poli, C. Detrembleur, *Chem. Eur. J.* **2008**, *14*, 7623-7637; b) A. Debuigne, R. Poli, J. De Winter, P. Laurent, P. Gerbaux, P. Dubois, J.-P. Wathelet, C. Jérôme, C. Detrembleur, *Chem. Eur. J.* **2010**, *16*, 1799-1811; c) A. Debuigne, R. Poli, J. De Winter, P. Laurent, P. Gerbaux, J.-P. Wathelet, C. Jérôme, C. Detrembleur, *Macromolecules* **2010**, *43*, 2801-2813; d) A. Debuigne, A. N. Morin, A. Kermagoret, Y. Piette, C. Detrembleur, C. Jérôme, R. Poli, *Chem. Eur. J.* **2012**, *18*, 12834–12844; e) A. N. Morin, C. Detrembleur, C. Jérôme, P. D. Tullio, R. Poli, A. Debuigne, *Macromolecules* **2013**, *46*, 4303–4312.
[7] A. W. Ehlers, M. Bohme, S. Dapprich, A. Gobbi, A. Hollwarth, V. Jonas, K. F. Kohler, R. Stegmann, A. Veldkamp, G. Frenking, *Chem. Phys. Lett.* **1993**, *208*, 111-114.
[8] A. W. Ehlers, M. Bohme, S. Dapprich, A. Gobbi, A. Hollwarth, V. Jonas, K. F. Kohler, R. Stegmann, A. Veldkamp, G. Frenking, *Chem. Phys. Lett.* **1993**, *208*, 237-240.
[9] S. Grimme, J. Antony, S. Ehrlich, H. Krieg, *J. Chem. Phys.* **2010**, *132*, 154104.
[10] M. Guerre, M. Semsarilar, F. Godiard, B. Ameduri, V. Ladmiral, *Polym. Chem.* **2017**, *8*, 1477-1487.
[11] a) K. Nakagawa, Y. Ishida, *J . Polym. Sci. Part B: Polym. Phys.* **1973**, *11*, 2153-2171; b) J. N. Martins, T. S. Bassani, R. V. B. Oliveira, *Mat. Sci. Eng. C* **2012**, *32*, 146-151.
[12] M. Pianca, E. Barchiesi, G. Esposto, S. Radice, *J. Fluorine Chem.* **1999**, *95*, 71-84.
[13] a) C. Boyer, D. Valade, L. Sauguet, B. Ameduri, B. Boutevin, *Macromolecules* **2005**, *38*, 10353-10362; b) E. B. Twum, C. Gao, X. Li, E. F. McCord, P. A. Fox, D. F. Lyons, P. L. Rinaldi, *Macromolecules* **2012**, *45*, 5501-5512.
[14] M. Guerre, G. Lopez, T. Soulestin, C. Totée, B. Améduri, G. Silly, V. Ladmiral, *Macromol. Chem. Phys.* **2016**, *217*, 2275-2285.
[15] a) G. Lopez, M. Guerre, J. Schmidt, Y. Talmon, V. Ladmiral, J.-P. Habas, B. Ameduri, *Polym. Chem.* **2016**, *7*, 402-409; b) G. Lopez, B. Ameduri, J.-P. Habas, *Macromol. Rapid Commun.* **2016**, *37*, 711-717.
[16] a) A. Manseri, B. Ameduri, B. Boutevin, R. D. Chambers, G. Caporiccio, A. P. Wright, *J. Fluorine Chem.* **1995**, *74*, 59-67; b) A. Manseri, B. Ameduri, B. Boutevin, R. D. Chambers, G. Caporiccio, A. P. Wright, *J. Fluorine Chem.* **1996**, *78*, 145-150.

Acknowledgements

Financial support from the French national agency (ANR grant FLUPOL) is greatly appreciated. C.D. and A.D. are Research Director and Research Associate by FNRS, respectively, and thank FNRS for financial support. We also thank Arkema company (Pierre-Bénite, France) for supplying VDF. This work was granted access to the HPC resources of CINES and IDRIS under the allocation (2006-2017)-086343 made by GENCI (Grand Equipement National de Calcul Intensif) and to the resources of the CICT (Centre Interuniversitaire de Calcul de Toulouse, project CALMIP).

Conflict of interest

The authors declare no conflict of interest.

Published in : Angewandte Chemie (2018), vol. 57, n°11, pp. 2934–2937
DOI: 10.1002/anie.201712347
Status : Postprint (Author's version)

References

[1] a) B. Améduri, *Chem. Rev.* 2009, 109, 6632–6686; b) D. W. Smith, S. T. Iacono, S. S. Iyer, *Handbook of Fluoropolymer Science and Technology*, Wiley, New York, 2014; c) A. D. Asandei, *Chem. Rev.* 2016, 116, 2244–2274; d) B. Ameduri, H. Sawada, *Fluorinated Polymers: From Fundamental to Practical Synthesis and Applications, Volume 1:Synthesis, Properties, Processing and Simulations*, Royal Society of Chemistry, Oxford, 2016.

[2] a) L. Yang, X. Li, E. Allahyarov, P. L. Taylor, Q. M. Zhang, L. Zhu, *Polymer* 2013, 54, 1709–1728; b) T. Soulestin, V. Ladmiral, B. Améduri, *Prog. Polym. Sci.* 2017, 72, 16–60.

[3] Z. Cui, E. Drioli, Y. M. Lee, *Prog. Polym. Sci.* 2014, 39, 164–198.

[4] F. Boschet, B. Améduri, *Chem. Rev.* 2014, 114, 927–980.

[5] a) M. Tatemoto in *The first Regular Meeting of Soviet-Japanese Fluorine Chemists*, Tokyo, 1979; b) M. Tatemoto, *Polymeric Materials Encyclopedia*, Vol. 5 (Ed.: J. C. Salamone), CRC Boca Raton, 1996, pp. 3847–3862; c) G. David, C. Boyer, J. Tonnar, B. Améduri, P. Lacroix-Desmazes, B. Boutevin, *Chem. Rev.* 2006, 106, 3936–3962; d) R. Vukicevic, U. Schwadtke, S. Schmucker, P. Schafer, D. Kuckling, S. Beuermann, *Polym. Chem.* 2012, 3, 409–414.

[6] a) G. Kostov, F. Boschet, J. Buller, L. Badache, S. Brandsadter, B. Am8duri, Macromolecules 2011, 44, 1841–1855; b) M. Guerre, B. Campagne, O. Gimello, K. Parra, B. Ameduri, V. Ladmiral, Macromolecules 2015, 48, 7810–7822; c) M. Guerre, S. M. W. Rahaman, B. Ameduri, R. Poli, V. Ladmiral, Polym. Chem. 2016, 7, 6918–6933.

[7] E. Girard, J. D. Marty, B. Am8duri, M. Destarac, ACS Macro Lett. 2012, 1, 270–274;

[8] M. Guerre, S. M. W. Rahaman, B. Ameduri, R. Poli, V. Ladmiral, Macromolecules 2016, 49, 5386–5396.

[9] A. D. Asandei, O. I. Adebolu, C. P. Simpson, J. Am. Chem. Soc. 2012, 134, 6080–6083.

[10] R. Liepins, J. R. Surles, N. Morosoff, V. T. Stannett, M. L. Timmons, J. J. Wortman, J. Polym. Sci. Polym. Chem. Ed. 1978, 16, 3039–3044.

[11] Z. C. Zhang, Z. M. Wang, T. C. M. Chung, Macromolecules 2007, 40, 5235–5240.

[12] a) W. Weng, Z. Shen, R. F. Jordan, J. Am. Chem. Soc. 2007, 129, 15450–15451; b) Z. Shen, R. F. Jordan, Macromolecules 2010, 43, 8706–8708; c) S. Wada, R. F. Jordan, Angew. Chem. Int. Ed. Angew. Chem. Int. Ed. Engl. 2017, 56, 1820–1824; Angew. Chem. 2017, 129, 1846–1850.

[13] D. Lanzinger, M. M. Giuman, T. M. J. Anselment, B. Rieger, ACS Macro Lett. 2014, 3, 931–934.

[14] a) R. Poli, Angew. Chem. Int. Ed. 2006, 45, 5058–5070; Angew. Chem. 2006, 118, 5180–5192; b) A. Debuigne, M. Hurtgen, C. Detrembleur, C. Jerome, C. Barner-Kowollik, T. Junkers, Prog. Polym. Sci. 2012, 37, 1004–1030; c) L. E. N. Allan, M. R. Perry, M. P. Shaver, Prog. Polym. Sci. 2012, 37, 127–156; d) A. Debuigne, C. Jerome, C. Detrembleur, Polymer 2017, 115, 285–307.

[15] A. Kermagoret, A. Debuigne, C. Jerome, C. Detrembleur, Nat. Chem. 2014, 6, 179–187.

[16] A. Debuigne, Y. Champouret, R. J8rkme, R. Poli, C. Detrembleur, Chem. Eur. J. 2008, 14, 4046–4059.

[17] A. Debuigne, J.-R. Caille, R. J8rkme, Macromolecules 2005, 38, 5452–5458.

[18] S. Banerjee, Y. Patil, T. Ono, B. Ameduri, Macromolecules 2017, 50, 203–214.

[19] R. Poli, S. M. W. Rahaman, V. Ladmiral, B. Ameduri, J. Organomet. Chem. DOI: 10.1016/j.jorganchem.2017.1012.1020.

[20] a) V. S. D. Voet, G. ten Brinke, K. Loos, J. Polym. Sci. Part A 2014, 52, 2861–2877; b) M. Guerre, M. Uchiyama, E. Folgado, M. Semsarilar, B. Ameduri, K. Satoh, M. Kamigaito, V. Ladmiral, Acs Macro Lett. 2017, 6, 393–398; c) M. Guerre, J. Schmidt, Y. Talmon, B. Ameduri, V. Ladmiral, Polym. Chem. 2017, 8, 1125–1128; d) M. Guerre, M. Semsarilar, F. Godiard, B. Ameduri, V. Ladmiral, Polym. Chem. 2017, 8, 1477–1487; e) M. Guerre, M. Semsarilar, C. Totee, G. Silly, B. Ameduri, V. Ladmiral, Polym. Chem. 2017, 8, 5203–5211.

[21] M. Destarac, K. Matyjaszewski, E. Silverman, B. Ameduri, B. Boutevin, Macromolecules 2000, 33, 4613–4615.

[22] A. Debuigne, C. Jerome, C. Detrembleur, Angew. Chem. Int. Ed.

[23] 2009, 48, 1422–1424; Angew. Chem. 2009, 121, 1450–1452. [23] J. Ahmad, M. B. H,gg, J. Membr. Sci. 2013, 445, 200–210.